A Marine Geophysical Study of the Wilkes Land Rifted Continental Margin, Antarctica

by

David I. Close

Thesis submitted for the Degree of Doctor of Philosophy, University of Oxford

Worcester College &
Department of Earth Sciences

Michaelmas Term 2004

A Marine Geophysical Study of the Wilkes Land Rifted Continental Margin, Antarctica

David I. Close

Worcester College & Department of Earth Sciences

Thesis submitted for the Degree of Doctor of Philosophy to the University of Oxford,

Michaelmas Term 2004

The Wilkes Land margin of East Antarctica, conjugate to the southern Australian margin, is a non-volcanic rifted margin that formed during the Late Cretaceous. During 2000-01 and 2001-02, Geoscience Australia (GA) acquired ∼10,000 line km of seismic reflection, magnetic anomaly, and gravity anomaly data, on the Wilkes Land margin.

Seismic reflection and sonobuoy refraction data provide the first constraints on sediment thickness and images of the deep crustal structure for the extent of the Wilkes Land margin. Two major post-rift seismic-stratigraphic sequences are recognised, separated by a regionally correlatable unconformity. The unconformity is interpreted as Early- to Middle-Eocene (∼50 Ma). This unconformity has previously been interpreted to represent the onset of continent-wide glaciation at ∼34 Ma. A major unconformity at the base of post-rift sediments is interpreted as a breakup unconformity, of approximately Turonian (85-90 Ma) age.

Timing the onset of seafloor spreading using lineated magnetic anomalies within the Australia-Antarctic Basin (AAB) is extremely difficult due to uncertainties in correlating anomalies to the geomagnetic reversal time scale. Modelling indicates that the anomaly commonly correlated to Chron 34y may, in some cases, be associated with high level intrusions and/or serpentinisation of exhumed upper-mantle peridotites.

Process-oriented gravity modelling indicates that the Wilkes Land margin lithosphere is characterised by a relatively high effective elastic thickness (T_e). Isostatic anomalies are most effectively reduced for models utilising T_e = 30 km. Although the margin is broadly characterised by a high T_e, zones of low T_e are inferred from modelling. Spectral analysis of isostatic anomalies indicates that the power of the flexural isostatic anomalies is lower than the free air gravity anomalies.

The margin does not appear to be segmented, at least in regard to its long-term strength. However, a change in initial, zero-elevation crustal thickness (T_c) is inferred from west to east. A T_c of ∼35 km is inferred for western Wilkes Land, whereas eastern Wilkes Land is characterised by T_c =29 to 31 km. Limited seismic refraction data from the conjugate margin indicates a similar trend from southwest to southeast Australia.

Extended Abstract

The Wilkes Land margin of East Antarctica, conjugate to the southern Australian margin, is a non-volcanic rifted margin that formed as a result of intracratonic extension within Gondwana during the Late Cretaceous. The present-day Wilkes Land margin is separated from southern Australia by the ∼3000 km wide southeast Indian and Southern Oceans, contained within the Australia-Antarctica Basin (AAB). The active spreading centre within the AAB is the South East Indian Ridge (SEIR), which is located approximately halfway between the opposing rifted margins.

The SEIR runs broadly east-west at ∼50°S as far east as 140°E, where it is offset to the south by a series of transform faults. A region of anomalously deep oceanic crust, the Australian-Antarctic Discordance (AAD), extends from the SEIR, between ∼120-130°E, to the north and south as far as the margins of Australia and Antarctica respectively. This depth anomaly has been interpreted to represent long-lived asthenospheric downwelling beneath the SEIR.

The morphology of the opposing margins of the AAB is vastly different. The differences reflect the disparate environmental conditions of the Antarctic and Australian continents through the Tertiary. The Wilkes Land margin comprises a rugged and overdeepened shelf associated with glacial erosion during times of glacial expansion. The southern Australian margin comprises a more typical shelf morphology, however, a prominent sediment terrace, the Ceduna Terrace, extends from the upper continental slope for over 100 km off the Great Australian Bight (GAB) margin. No similar terraces are apparent on the conjugate central Wilkes Land margin.

Recently acquired deep-penetrating seismic reflection, sonobuoy refraction, magnetic anomaly, and gravity anomaly data have allowed the structure and evolution of the Wilkes Land margin to be investigated in detail. Interpretation and modelling, where appropriate, of these data provides insights into the age, crustal structure, seismic stratigraphy, subsidence history, and thermo-mechanical evolution of the Wilkes Land margin.

Seismic reflection data, supplemented by sonobuoy refraction data, provide the first constraints on sediment thickness and images of the deep crustal structure for the extent of the Wilkes Land margin. Two major post-rift seismic-stratigraphic sequences are

recognised, separated by a regionally correlatable unconformity. This unconformity is recognised beneath the continental slope and rise by the erosional truncation of underlying strata, and the onlap of overlying reflectors. The unconformity is interpreted as Early- to Middle-Eocene (∼50 Ma) on the basis of correlation with seismic reflection and subsidence data from the conjugate southern Australian margin. This unconformity has previously been interpreted to represent the onset of continent-wide glaciation at ∼34 Ma.

The upper post-rift stratigraphy (Sequence 1) records the change from temperate climatic conditions, to temperate-glacial and then polar-glacial conditions; a major event that was the catalyst for a shift in global climate patterns towards the present-day *ice-house* conditions. No single stratigraphic feature can be correlated with the onset of regional glaciation and the development of the East Antarctic Ice Sheet (EAIS). However, the great thickness of Sequence 1 sediments in some areas (>9 km) is likely an indication of continental erosion and sediment transport, associated with wet-based glaciers, prior to the development of polar-glacial conditions.

An approximately seven-fold reduction in sedimentation rates in the Late Miocene (∼9 Ma) is interpreted to represent the onset of stable, frozen-based, polar glaciers. Inferred sedimentation rates for the ∼34-9 Ma interval are comparable to the highest present-day, observed sedimentation rates at continental margins. Sequence 1, therefore, represents a large load on the rifted Wilkes Land margin lithosphere that was deposited relatively rapidly some 60-80 Ma after rifting.

The Sequence 1 isopach indicates the presence of a major sedimentary basin off the west Wilkes Land margin. The asymmetric distribution of sediments within this basin indicates long-lived west to east sediment transport processes have operated on the Wilkes Land margin continental rise. Present-day observations of deep-marine currents, however, do not indicate the presence of a strong eastward current off the Wilkes Land margin. This may suggest that ocean circulation has changed significantly since the development of polar-glacial conditions.

A major unconformity at the base of Sequence 2 is interpreted as a breakup unconformity, of approximately Turonian age, on the basis of correlation with seismic and well data from the southern Australian margin. The unconformity represents the base of relatively undeformed and unfaulted reflectors for the western and central Wilkes Land margin. However, off eastern Wilkes Land and Terre Adélie, extension-related deformation and faulting is interpreted to have continued until the Early Tertiary. The first evidence of oceanic crust occurs over 400 km from the shelf break off this margin sector, ∼200 km further seaward than off central Wilkes Land. A bathymetric shallowing and cluster of seamounts off eastern Wilkes Land corresponds to this region of heavily

extended continental crust. This region has previously been interpreted as a zone of anomalous oceanic crust.

Underlying the post-rift sediments on the Wilkes Land margin is a combination of extended and deformed continental crust, transition zone crust (typically comprising a number of acoustically transparent basement highs), and oceanic crust. Continental crust is identified on the basis of rotated fault blocks and tilted reflectors in the upper-crust, and a massively thinned, acoustically transparent lower crust that terminates at the landward edge of transitional crust. Oceanic crust exhibits relatively rugged topography, an upper surface characterised by a high-amplitude reflector, and an acoustically transparent internal character. Sonobuoy data indicate that oceanic crust at the Wilkes Land margin comprises a reduced layer 3 thickness and is only ~75% the thickness of *normal* (i.e. Atlantic and Pacific Ocean) oceanic crust.

The exact breakup age of Australia and Antarctica is difficult to constrain. Subsidence analyses from the southern Australian margin identify two intervals of tectonic subsidence, the younger of which, in the Late Cretaceous, is interpreted to relate to breakup. Accurately timing the onset of seafloor spreading using lineated magnetic anomalies, however, is extremely difficult due to uncertainties in correlating anomalies to the geomagnetic reversal time scale. Initial opening at the incipient SEIR proceeded at very low spreading rates (<10 mm/yr Half Spreading Rate - HSR), which, in combination with hydrothermal alteration associated with sediment blanketing of young, hot oceanic crust, resulted in a poor record of magnetic reversals in Late Cretaceous and Palaeocene aged oceanic crust in the AAB.

The oldest previously interpreted seafloor spreading magnetic anomaly is associated with the end of the Long Cretaceous Normal Polarity period, Chron 34 (i.e. anomaly 34y). However, the form of this anomaly is inconsistent within the AAB and is located within the COT interpreted in seismic reflection data. Magnetic modelling, constrained by the depth to basement interpreted from seismic reflection data, indicates that the anomaly commonly correlated to Chron 34y may, in some cases, be associated with high level intrusions and/or serpentinisation of exhumed upper-mantle peridotites.

It is clear, from interpretation of magnetic anomaly data, that breakup was not synchronous along the length of the SEIR. The lack of recognisable seafloor spreading anomalies older than Chron 21 in the eastern AAB, which correlates to the region of anomalous extension identified in seismic reflection data, indicates that final breakup did not occur there until the Eocene (~50 Ma). The emplacement of oceanic crust in the eastern AAB correlates to a basin-wide increase in seafloor spreading rates. This change in spreading rates is interpreted to correlate to an increase in thermal subsidence rates identified from well data on the southern Australian margin, and is likely the catalyst for

development of the major unconformity that punctuates the post-rift seismic sequence. Seafloor spreading is interpreted to have remained relatively fast (20-38 mm/yr HSR) since the Eocene, and the associated lineated magnetic anomalies can be confidently correlated to the geomagnetic reversal time scale.

Two-dimensional process-oriented gravity modelling, using depth-converted sediment thickness data, reveals that the Wilkes Land margin lithosphere is characterised by a relatively high effective elastic thickness (T_e). Isostatic anomalies are most effectively reduced for models utilising T_e = 30 km. Process-oriented modelling is most sensitive to T_e variation off west Wilkes Land where the thickest post-rift sediments are located. Although the margin is broadly characterised by a high T_e, zones of low T_e are inferred from modelling. This likely indicates that some sections of extended continental crust were weakened by rifting processes and have not recovered strength equivalent to the relatively unstretched, adjacent continental crust. Multi-layer backstripping does not provide any evidence of major temporal variation in T_e. However, due to the greater relative thickness of Sequence 1 it is difficult to determine this from studies of lithospheric loading.

Three-dimensional modelling also indicates a relatively high T_e for the Wilkes Land margin lithosphere. Isostatic anomalies associated with thick sediments and the continental edge effect are most effectively reduced for models created assuming $T_e = 30 to 45$ km. Spectral analysis of isostatic anomalies indicate that the power of the flexural isostatic anomalies is lower than the free air gravity anomalies.

The margin does not appear to be segmented, at least in regard to its long-term strength. However, a change in initial, zero-elevation crustal thickness (T_c) is inferred from west to east. A T_c of $\sim$35 km is inferred for western Wilkes Land, whereas eastern Wilkes Land is characterised by T_c =29 to 31 km. Limited seismic refraction data from the conjugate margin indicates a similar trend from southwest to southeast Australia.

Process-oriented gravity modelling has also been undertaken on the southern Australian margin. Results broadly indicate a lower T_e relative to the Wilkes Land margin. This is interpreted to indicate that sediment loading in the Late Cretaceous occurred on weakened lithosphere, and that backstripping studies recover this lower T_e because there has been relatively little subsequent loading throughout the Tertiary. Whereas, the major sediment loading interval on the Wilkes Land margin occurred some 60-80 Ma after rifting. This is the first evidence from a conjugate margin pair that continental lithosphere increases in strength following rifting.

Spatially correlated flexural isostatic and free air anomalies, magnetic anomalies, and basement features interpreted in seismic reflection data are observed. On the basis of forward modelling and inversion, these features are interpreted to have a density of

$\sim$3100 kg/m^3, and high magnetic susceptibility. Serpentinised upper-mantle peridotites are inferred on the basis of these results. Upper mantle peridotites have been dredged from a seamount-scarp offshore from eastern Wilkes Land, and similar structures have previously been inferred on the southern Australian margin.

Comparison of seismic reflection data indicate a broad-scale symmetry between the conjugate margins. Additionally, large-scale detachments are not imaged in seismic reflection data, therefore they do not support the lower plate and upper plate margin classifications of simple shear models. Greater depth of bathymetry off the southern Australian margin relative to the Wilkes Land margin is primarily a function of the different Tertiary sedimentation histories of the margins. The gravity and magnetic anomaly sequences are broadly symmetric also.

Depth anomalies of up to 800 m, calculated for the sediment unloaded oceanic crust, confirm greater depths of Wilkes Land oceanic crust relative to that expected from global ocean depth-age trends. This is likely a function of the initially greater depth of oceanic crust extruded at the SEIR, and in particular the AAD. The depth anomalies are not apparent for the possible seafloor spreading anomaly 34y, and for one location the backstripped basement is shallower than the depth predicted for oceanic crust for this anomaly. This provides further evidence that the anomaly previously identified as 34y may not be associated with *normal* oceanic crust.

This thesis provides insight into the evolution of a previously relatively unexplored, frontier, rifted continental margin. The interpretation and modelling results place the Wilkes Land margin in a regional and global context and indicate that it is anomalous with regards to its high lithospheric rigidity. The identification of a sunken marginal plateau or micro-continent off eastern Wilkes Land is important in understanding the breakup and dispersal history of southeast Australia, Tasmania and its associated micro-continents, and eastern Wilkes Land and northern Victoria Land of Antarctica.

Declaration

I hereby declare that this thesis, submitted in fulfilment of the requirements for the degree of Doctorate of Philosophy, represents my own work and is less than 80,000 words in length. This work has not been previously submitted to this or any other institution for any degree, diploma or other qualification.

David I. Close

Acknowledgements

I would like to acknowledge the supervision of Tony Watts over the past three years, particularly for the thorough reviews of this thesis in recent months. I would also like to thank my co-supervisor, Howard Stagg, and the staff of Geoscience Australia for their help, particularly Jim Colwell, Phil Symonds and Fred Kroh.

Many individuals, outside of Oxford, have contributed to various aspects of this project. In particular I would like to thank Takemi Ishihara (JNOC), Jon Childs (USGS), Rob Larter (BAS), Andrew Goodwillie and Bob Fisher (GEBCO), Fred Kroh (GA), all members of the GA Law of the Sea team and Jennie Totterdell, and Nick Direen (Uni. of Adelaide). The financial support of the Rhodes Trust and Shell are also acknowledged.

I would like to thank the staff of the Department of Earth Sciences for helping at every point possible during this project. Thank you also to all the graduate students for providing the high points of each day during the morning and afternoon coffee breaks. In particular I would like to thank my fellow members of the Marine Group over the past three years, especially Natalie Lane, Tiago Cunha, Tom Jordan and Matt Rodger for reading early drafts of several chapters. I would also like to thank Paul Wyer, Mohammed Ali, Marta Perez-Gussinye and John Hillier for discussions on all things marine and geophysical. The assistance of Steve Usher has also been invaluable everytime the computers misbehaved.

Images within this thesis have almost entirely been created using the GMT software of P. Wessel and W. Smith (http://www.soest.hawaii.edu/gmt).

On a personal note, I would like to thank all my friends at Oxford for making my time here so enjoyable. Thankfully, they are too numerous to name individually here. I would particularly like to thank the lovely Eliana, who has been so patient with me over the last year! Lastly, but by no means not least, I want to give huge thanks to my family for all their support over the past 25 years, I would never have got here without them.

Contents

List of Figures

List of Tables

Glossary of terms and abbreviations

The following terms, abbreviations and acronyms are used throughout this thesis.

AAB	Australia-Antarctic Basin
AAD	Australia-Antarctic Discordance
ABC	Aurora Basin Complex
AGC	Automatic Gain Control
ARB	Adelie Rift Block
BAS	British Antarctic Survey
COB	Continent-Ocean Boundary
COT(Z)	Continent-Ocean Transition (Zone)
CMP	Common Midpoint Point
CTB	Continent-Transition Boundary
D_c	Depth of compensation
DSDP	Deep Sea Drilling Program
E	Young's modulus
EAIS	East Antarctic Ice Sheet
EOC	Eocene aged unconformity
FAA	Free-Air Gravity Anomaly
FFID	Field File ID
FFT	Fast Fourier Transform
FIA	Flexural Isostatic Anomaly
FZ	Fracture Zone
g	Gravitational acceleration
G	Gravitational constant
GA	Geoscience Australia
GAB	Great Australian Bight
GMT	Generic Mapping Tools (http://www.soest.hawaii.edu/gmt)
GPS	Global Positioning System

IFP	Institut Francais du Petrole
JNOC	Japanese National Oil Company
KLNP	Cretaceous Long Normal Polarity period
LLCC	Laminated Lower Continental Crust
MCS	Multi-Channel Seismic
MOR	Mid-Ocean Ridge
MORB	Mid-Ocean Ridge Basalt
MQZ	Magnetic Quiet Zone
MSL	Mean Sea Level
NMO	Normal Move-Out
ODP	Ocean Drilling Program
Q	Königsberger Ratio
QZB	Quiet Zone Boundary
RMS	Root Mean Square
SB	Sonobuoy
SCAR	Scientific Committee on Antarctic Research
SDLS	Seismic Data Library Service
SDR	Seaward Dipping Reflector
SEG-Y	Trace sequential seismic recording standard
SEIR	Southeast Indian Ridge
SP	Shot Point
SRS	Southern Rift System
STR	South Tasman Rise
t	Time
T	Temperature
TAM	Transantarctic Mountains
T_c	Zero elevation, initial continental crustal thickness
T_e	Effective elastic thickness of the lithosphere
Tran	Reflector at top of transparent lower crust
TRM	Thermo-Remanent Magnetisation
T_s	Seismogenic thickness
TTS	Total Tectonic Subsidence
Tur	Turonian aged unconformity
TWT	Two-Way Time
USGS	United States Geological Survey
UNCLOS	United Nations Commission on the Law of the Sea

V	Velocity
V_p	P-wave velocity
W	Deflection (flexure)
WEMR	Wave Equation Multiple Rejection
WL	Wilkes Land
YSE	Yield Stress Envelope
Z_{neck}	Depth of Necking
λ	Wavelength
ρ	Density
σ	Poisson's ratio

Units

dB	Decibels
Hz	Hertz
km	kilometre
m	metres
Ma	10^6 years before present
mm	millimetre
ms	millisecond
My	10^6 years
nT	nanoTesla
s	second
yr	year

Chapter 1

Introduction

1.1 Continental Margins

1.1.1 Introduction

The term continental margin describes the region that separates the thick, geologically complex crust of the continents from the relatively thin, less structurally complex and compositionally diverse crust of oceanic basins. Continental and oceanic crust exhibit mean elevations of +0.8 km and -3.7 km relative to sea level, respectively [Kennett, 1982], the continental margin is, therefore, also a prominent morphologic feature.

Suess [1904] recognised that the morphology and geology of continental margins varied greatly, and introduced the descriptive terms, Atlantic margin and Pacific margin. The classifications of Suess [1904] are based on the fundamental differences between the wide coastal plains and thick sediments at the margins of the Atlantic Ocean, and the folded mountain belts, island arcs, volcanism and seismic activity at the margins of the Pacific Ocean.

The Suess [1904] classification of Pacific and Atlantic type margins remains in use today, although a large number of genetically descriptive terms are now also used to describe these margin types. A third major type of continental margin is recognised today, the Transform margin. The differentiation between the major margin types is a function of their relation to plates, plate boundaries, and the presence or absence of seismic and/or volcanic activity. Other common terms for Pacific, Atlantic and Transform type margins are:

- Atlantic: divergent, passive, or rifted.
- Pacific: convergent or active.
- Transform: translational or sheared.

The worldwide distribution of rifted, convergent and transform margins is illustrated in Figure 1.1.

We concentrate here on rifted margins. Rifted margins are old plate edges formed by the extension and eventual *breakup* of continental crust and the emplacement of oceanic crust. *Breakup*, is used here to describe the rifting and drifting stages of continental

Figure 1.1: Worldwide distribution of rifted (divergent), convergent, and transform margins. After Emery [1980].

fragmentation, it is associated with the first generation of new oceanic crust and the initiation of seafloor spreading. Hence, the rifted margin marks the transition to active rifted plate tectonic processes and the formation of an ocean basin. Physiographically, rifted margins are typified by the following conventional morphologic demarcations, after Heezen [1974]. Although such classifications are overly simplistic they provide a term of reference and comparison.

- Continental shelf, the gently dipping region of little relief extending from the coast to the *shelf break*, where the seafloor steepens and the continental slope begins.

- Continental slope, the region where gradients range from 20-4%. In some regions, such as northwest Australia and southeast South America, a *marginal plateau* at a depth of 800-1000 m lies between the continental shelf and slope.

- Continental rise, where typical gradients do not exceed 1%. In some areas the low relief of the continental rise is punctuated by large seamounts or seamount groups, some reaching elevations greater than sea level (e.g. Cape Verde Islands, The Canary Islands).

- Abyssal plain, gradients on the abyssal plain are generally less than 0.1% (a change in microtopography is also characteristic of the abyssal plain regions).

Rifted margins are generally characterised by a wide continental shelf relative to Pacific and Transform type margins. Another common characteristic of rifted margins are submarine channel systems, which dissect the continental shelf and slope regions. These features are associated with the transport of terrigenous sediment, and its subsequent erosion of and deposition on the continental slope and rise. The shelf break varies in depth

as a function of latitude at rifted margins [Heezen, 1974]. Shelf break depths commonly exceed 500 m in polar regions, whereas in more temperate latitudes the average depth is ∼130 m [Kennett, 1982]. This difference is primarily a result of glacial activity at higher latitudes. Shelf *over-deepening* associated with erosion by glaciers or ice-berg keels during times of glacial advance across the continental shelf is considered the primary cause of the greater depth of the shelf break at high latitudes (e.g. and Barnes [1987], Anderson [1991]). However, flexural downwarping, due to ice sheet loading, also contributes to shelf over-deepening (e.g. ten Brink *et al.* [1995]). A bathymetric profile through the Southern and southeast Indian Oceans between Antarctica and Australia (Figure 1.2) illustrates the morphological regions typical of rifted margins.

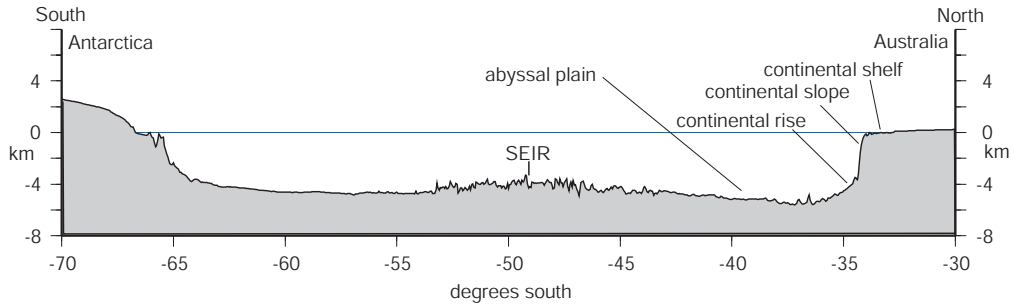

Figure 1.2: Bathymetric transect of the Southern and southeast Indian Oceans, between East Antarctica and southern Australia, at 130°E. SEIR = southeast Indian Ridge.

1.1.2 Structure of Rifted Margins

Crust, Sediment, and Magmatism

The continental crust underlying a rifted margin can be observed in seismic data to thin seawards (e.g. De Charpal *et al.* [1978], Hutchinson *et al.* [1982]). The transition to oceanic crust can occur over a few tens of km up to more than 150 km [Dean *et al.*, 2000]. Continental, cratonic crust at rifted margins is typically altered by stretching, faulting and igneous intrusive activity. However, this deformed crust remains distinct in chemical, structural and geophysical properties from oceanic crust.

Despite the differences in the nature of the crustal types underlying continental margins, the Continent-Ocean Boundary (COB) is an enigmatic geological feature. Geological factors, such as thick sedimentary sequences and masking lithologies (e.g. carbonates, salt, flood basalts) hinder the detailed seismic imaging of underlying crustal features, and typically prevent an absolute determination being made with seismic data alone. Interpretations based on other geophysical data are also rarely unambiguous.

Sedimentary sequences of great thickness, overlying rifted continental and oceanic

crust, occur at many rifted margins, e.g. northeast U.S.A [Hutchinson *et al.*, 1982]. However, some rifted margins are relatively sediment starved and comprise thin sedimentary sequences only, e.g. Hatton Bank [Fowler *et al.*, 1989]. The variations in sediment thickness are primarily a function of climatic conditions and uplift history of adjacent continental areas. Figure 1.3 shows a compilation of bathymetry and sediment thickness at a number of rifted margins, along with the free air gravity anomalies across the margins.

The sedimentary sequence at rifted margins is typically divided into three main units, *pre-rift, syn-rift*, and *post-rift*, as shown in Figure 1.4. The pre-rift sequence describes the deformed and faulted formations that predate rifting. Block rotation along listric normal faults is common within the pre-rift sequences (e.g. Moore *et al.* [2000]). Syn-rift sediments are deposited during active extension, crustal thinning and fault-controlled or tectonic subsidence. They are typically represented by dipping reflectors within fault-bounded rift basins. Rift basins often take the form of half-grabens and syn-rift sediments contained within them are often recognised by reflector divergence (associated with increasing sediment thickness) towards the bounding fault footwall (e.g. Krawczyk *et al.* [1996]). Fault-bounded rift basins and syn-rift sediments are normally blanketed with seaward-dipping, prograded and gently dipping to horizontal, aggraded clastic and carbonate sequences. The base of the post-rift sequence is often clearly marked by a *breakup unconformity* (e.g. Falvey [1974]). Post-rift sediments are typically undeformed and sparsely faulted, as they are deposited during an interval of thermal subsidence (e.g. McKenzie [1978]).

Although most rifted margins exhibit similar sedimentary characteristics, they differ markedly with regards to evidence of magmatic activity during margin evolution. Many margins exhibit evidence of excessive, transient magmatic activity during the final stages of breakup; these are classified as volcanic margins (e.g. Mutter *et al.* [1982], [Eldholm *et al.*, 1995]). Of all rifted margins around the world, 90% are volcanic rifted margins to varying degree, the exceptions being the rifted margins of eastern China, Iberia, the northern Red Sea, southern Australia, the Newfoundland Basin-Labrador Sea, and possibly the Gulf of California [Menzies *et al.*, 2002]. The margins of Antarctica are largely unknown with regards to evidence of rift-related magmatism.

Massive extrusive complexes along rifted margins were first recognised at the Vøring margin of Norway due to the smooth acoustic basement near the COB [Talwani & Eldholm, 1972]. The existence of wedges of seaward dipping, intrabasement reflectors below acoustic basement was later identified (e.g. Eldholm *et al.* [1979]). These Seaward Dipping Reflector (SDR) sequences are commonly used as the basis of identifying volcanic rifted margins (e.g. Coffin & Eldholm [1994]). The global distribution of volcanic margins

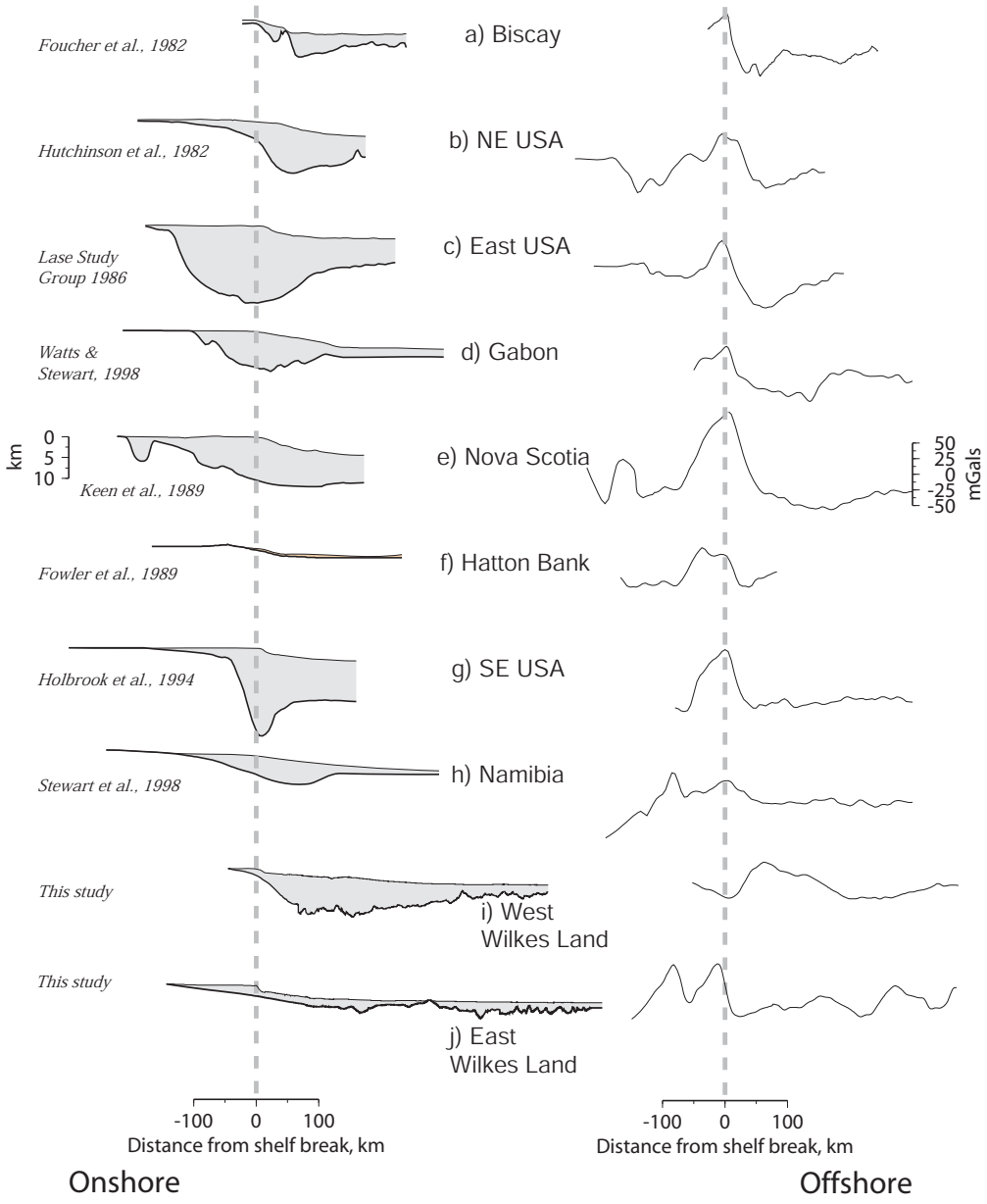

Figure 1.3: (a)-(h)Compilation of published profiles of upper crustal structure, with the grey-shaded area showing the undifferentiated thickness of volcanic and rift sediments above basement, and observed free air gravity anomalies at a number of margins worldwide. (i)-(j) Similar profiles across the western and eastern Wilkes Land margin from this study to enable comparison. Profiles are aligned on the shelf break. References Biscay [Foucher *et al.*, 1982]; USGS32, Carolina Trough [Hutchinson *et al.*, 1982]; LASE 6, Baltimore Canyon Trough [LASE Study Group, 1986]; Gabon [Watts & Stewart, 1998]; Nova Scotia [Keen *et al.*, 1990]; Hatton Bank [Fowler *et al.*, 1989]; EDGE801, US middle Atlantic margin [Holbrook *et al.*, 1994].

Figure 1.4: Seismic reflection section from the Otway Basin, southern Australia, divided into pre-, syn-, and post-rift sequences. After Moore *et al.* [2000].

based on wedges of intrabasement SDR is illustrated in Figure 1.5.

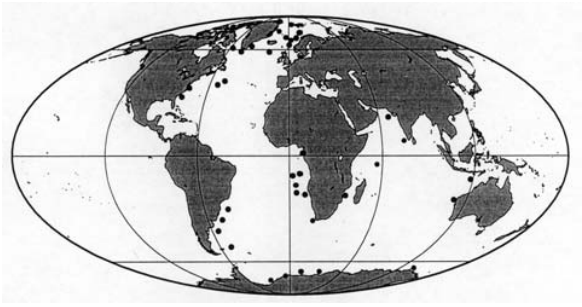

Figure 1.5: Global distribution of volcanic margins based on wedges of intrabasement seaward dipping reflectors, after Eldholm *et al.* [1995].

Eldholm *et al.* [1995] suggested that whether a volcanic margin develops or not during rifting depends on the temperature and fluid content of the asthenosphere along the

incipient plate boundary and the dynamic history of the lithosphere. They recognise a number of geological features by which volcanic margins can be identified, in addition to the commonly used seaward dipping reflector sequences. These include:

1. Onshore continental flood basalts.
2. Voluminous extrusive basaltic complexes along the continent-ocean transition appearing as intrabasement reflectors.
3. Sills and low-angle dikes within pre-rift sediments.
4. Thicker than normal oceanic crust adjacent to the COB.

The presence of thickened crust, commonly referred to as an *underplate*, is a common, but not universal, feature at volcanic rifted margins Eldholm *et al.* [1995]. Figure 1.6 illustrates some of the key geological features used to identify volcanic and non-volcanic margins. The identification or lack of these features allow volcanic margins to be distinguished from non-volcanic rifted margins.

1.1.3 Segmentation and Symmetry

Segmentation can be observed in bathymetry and marine gravity compilations to be a characteristic feature of seafloor spreading along the global mid-ocean ridge system. However, the processes by which an incipient rift and spreading centre develops into a segmented mid-ocean ridge, and how they relate to observed margin segmentation in the present-day is poorly understood [Behn & Lin, 2000].

At slow spreading rates, mid-ocean ridges are known to be highly three-dimensional, with segmentation observed both at active spreading centres and in aged oceanic crust by the presence of fracture zones and off-axis traces of nontransform offsets (e.g. Tucholke & Lin [1994]). In contrast, magma supply at fast spreading ridges, such as the East Pacific Rise, appears to be more two-dimensional [Lin & Phipps Morgan, 1992].

Cochran & Martinez [1988] identify segmentation of both the axial valley of the Red Sea rift basin and its margins on the basis of faulting and basaltic intrusive activity. The identification of segmentation at the axial valley and margins is interpreted to indicate that segmentation has been present in the Red Sea rift since its inception. Segmentation has also been inferred for the West African margin by Watts & Stewart [1998]. The identification of 350-400 km weak zones along-strike of the Gabon margin was interpreted by Watts & Stewart [1998] to indicate that rift margins may be highly segmented as regards their long-term strength. Structural segmentation has also been inferred on the Angolan margin by Hudec & Jackson [2002], where transfer zones associated with breakup are recognised as focal points for post-rift tectonism. Behn & Lin [2000] infer segmentation of the northeast U.S.A margin on the basis of gravity and magnetic anomaly

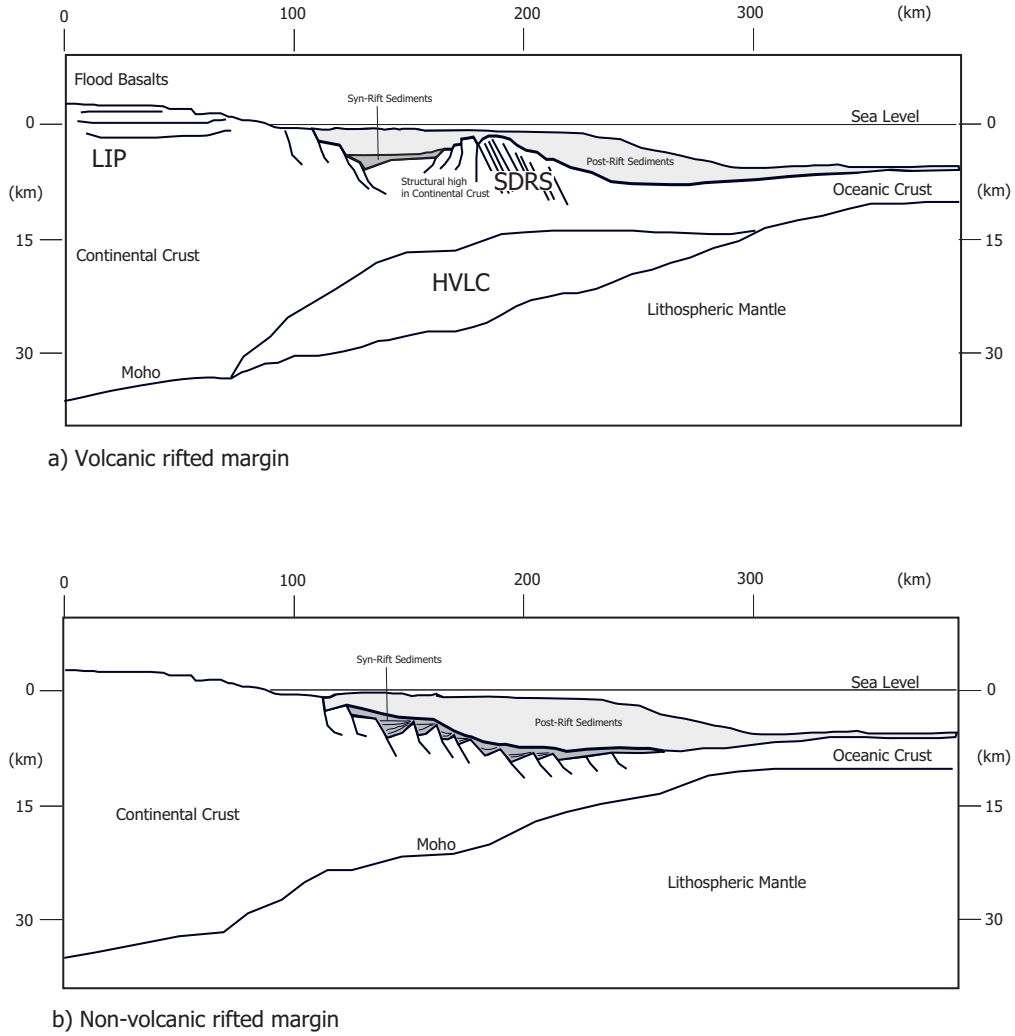

Figure 1.6: a) Schematic volcanic rifted margin. Volcanic rifted margins are characterised by a subaerial flood basalt province (i.e. large igneous province [LIP]) with upper and lower crustal magmatic systems; development of high-velocity lower crust (HVLC) in the transition from continental to oceanic domains; and, formation of a submarine, Seaward Dipping Reflector (SDR) sequence. After Menzies *et al.* [2002] and Symonds *et al.* [2000]. b) Schematic non-volcanic rifted margin. A lack of SDR allows the listric faulting within the rifted continental crust to be imaged in seismic reflection data.

character. They too imply that segmentation observed at mature spreading centres may be directly linked to segmentation during rifting and breakup.

If margin segmentation is related to processes at incipient spreading centres, then such segmentation should be relatively symmetrical for conjugate margin pairs. There is not yet sufficient evidence to determine if this is the case. The symmetry of conjugate margin pairs, however, has been the subject of much debate. Whether conjugate

margins exhibit symmetry with regards to degree of extension, width of extended crust, and lithosphere-scale deformation remains controversial. Pure shear models predict symmetric margins, whereas simple-shear or coupled pure and simple shear models predict asymmetric conjugate margins. Determining which model is more applicable is not trivial. For example, Etheridge *et al.* [1989] interpreted asymmetry between the southern Australia-East Antarctic conjugate margin pair and, therefore, inferred that breakup followed a simple shear process. However, the evidence cited by Etheridge *et al.* [1989] was discounted by Sayers *et al.* [2001] and the interpretation of a simple shear breakup questioned.

1.2 Continental Rifting and Rift Models

Buck *et al.* [1999] observed that *"...the more closely we look at areas of continental extension the more we see that all rifts are not created equal"*. As diverse as the variation in observed structure of rifted margins are the models that seek to explain observed data at these margins. A brief review of a number of the historically important rift models and their assumptions and/or application is given here.

McKenzie [1978] provides a relatively simple, pure shear model of continental extension and rifting. In this model, a section of uniform thickness lithosphere is instantaneously and uniformly extended by a stretching factor, β (Figure 1.7). Crustal thinning associated with the stretching causes an initial subsidence to maintain isostatic equilibrium. Lithospheric thinning in this model also creates an initial temperature perturbation that decays with time according to one-dimensional heat conduction, causing the continued and gradual thermal subsidence of the thinned crust. This model predicts a perfectly symmetrical rift basin (Figure 1.8a) and has been successfully applied in the modelling of many rift basins. However, it assumes a state of local isostasy, and therefore no lithospheric strength, is maintained during extension and rifting.

Wernicke [1985] suggested that subsidence across a rifted margin occurs as a result of simple shear along a low-angle detachment that extends through the crust and lithospheric mantle (Figure 1.8b). In this simple shear model the relative extension of crust and mantle lithosphere is non-uniform along any vertical line. Therefore, this model predicts asymmetric rifting and two broad classes of rifted margins; upper plate margins in the hanging wall of the detachment and lower plate margins in the footwall. A mixed-mode model of extension suggested by Kusznir & Park [1987] invokes brittle faulting above a detachment in the upper lithosphere accompanied by pure shear in the lower lithosphere (Figure 1.8c).

Weissel & Karner [1989] modelled the response of an elastic plate to isostatic forces

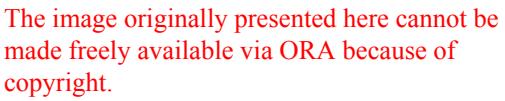

Figure 1.7: Sketch of the principal structural and thermal features from the McKenzie [1978] model of crustal extension, subsidence, and basin formation. β = stretching factor, C = crust, L = lithosphere, A = asthenosphere, a = thickness of the lithosphere.

Figure 1.8: Models of lithospheric extension. a) Symmetrical extension by pure shear, e.g. McKenzie [1978]. b) Asymmetrical extension by simple shear along a low-angle detachment. The thinnest part of the upper lithosphere is offset from the thinnest portion of the lower lithosphere. c) Mixed-mode extension. The lithosphere is cut by a dipping shear zone. Brittle faulting occurs above the detachment; ductile flow takes place at deeper levels. From Jones [1999] after Keen *et al.* [1989].

associated with a simple shear, Wernicke [1985] type, rift. Ebinger *et al.* [1991] applied such a model to explain the observed topography and gravity anomalies of the Western Rift of East Africa, where asymmetry in rift structure is observed. Models of this type have been labelled *flexural cantilever* models by Kusznir & Egan [1990]. In models of this type the lithosphere implicitly retains a finite rigidity during rifting.

Evidence from the continents and oceans suggest that lithospheric strength provides important constraints on crustal structure and, therefore, may influence rift processes. Changes in crustal thickness (i.e. the degree of stretching, β) and in the thickness of the mechanical lithosphere occur across rift margins. This necessarily alters the strength-depth relationships in continental lithosphere, and therefore also the yield strength envelope (YSE).

The YSE is a strength profile of the lithosphere that takes into account brittle and ductile deformation laws based on data from experimental rock mechanics (Figure 1.9). The strength profile increases linearly with depth and then decreases. The increase is given by Byerlee's Law, which varies for tension and compression. The decrease is given by ductile flow laws, which depend on the magnitude of the applied stress and the geotherm. The rate at which extension progresses, the thermal conditions, and mineralogical composition control YSE changes during rifting. Typically, thinned crust exhibits shallower and weaker, crust- and lithosphere-scale strength maxima [Wyer, 2003].

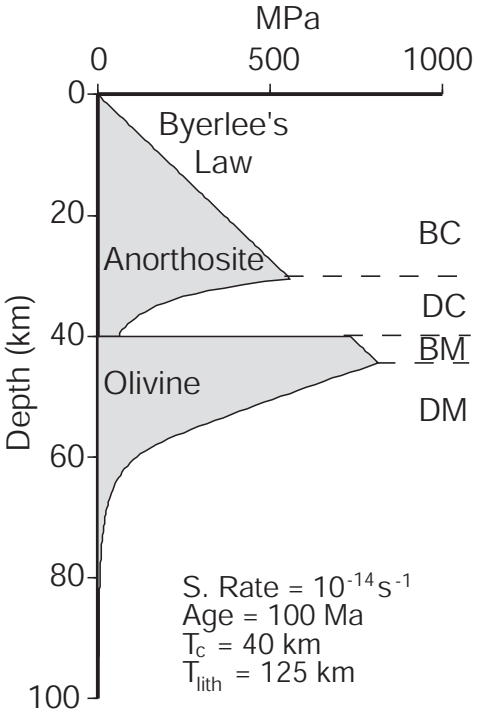

Figure 1.9: Yield Strength Envelope (YSE) profile for continental lithosphere assuming a "standard model" and an anorthosite crust and olivine mantle. The standard model is based on the strain rate (S.Rate), age, crustal thickness (T_c), and lithospheric thickness (T_{lith}) as labelled. BC and DC are brittle and ductile crust respectively, and BM and DM are brittle and ductile mantle respectively. After Watts [2001].

Modelling by Braun & Beaumont [1989] demonstrated that extension was concentrated preferentially at the depth of the maximum yield strength. Kooi *et al.* [1992] introduced the *depth of necking* model, based on the work of Braun & Beaumont [1989], which adapts the rift model of McKenzie [1978] by removing the assumption of Airy isostasy during rifting and allowing the lithosphere to thin preferentially at a depth of necking (Z_{neck}).

A major problem with the depth of necking model, however, is the assumption that Z_{neck} remains constant for the rift duration. Burov & Poliakov [1995] find that mechanical and thermal changes during rifting can cause necking to localise simultaneously and/or successively at multiple depths. Numerical modelling (e.g. Bassi [1995]), and laboratory scale analogue modelling (e.g. Brun & Beslier [1996] and Michon & Merle [2003]), of the rifting of a four layer lithosphere also demonstrate that the depth of the crustal, rheology based, strength maximum is non-constant during rifting (Figure 1.10).

Figure 1.10: Line drawing of an extending lithosphere analogue model composed of sand (brittle layers) and silicon (ductile layers), after Brun & Beslier [1996]. The model is based on rheological yield strength considerations and comprises four layers; Bc = brittle crust, Dc = ductile crust, Bm = brittle mantle, and Dm = ductile mantle.

The rheology based, four layer lithosphere models of Bassi [1995], Brun & Beslier [1996] and Michon & Merle [2003], comprise a plastic/brittle upper crust, a viscous/ductile lower crust, a plastic/brittle upper mantle, and viscous/ductile mantle (Figure 1.10). An important result of Brun & Beslier [1996] is the observation of both pure and simple shear in the same model rift system, although on different scales. They interpret lithospheric necking in their models to indicate pure shear at regional scales. However, within this essentially pure shear environment, they interpret shear components of opposing sense develop at the rheological interfaces within the crust and mantle.

The laboratory analogue experiments of Brun & Beslier [1996] and Michon & Merle

[2003] also indicate the presence of shear zones that control the overall, lithosphere scale thinning and necking. Brun & Beslier [1996] suggest that the final geometry of crustal layers is controlled by the rupture of the brittle mantle layer. The geometry and width of the rift system is also suggested to be a function of extension rate, with lower rates characterised by the formation of a single, asymmetric graben (narrow rift), and higher rates leading to the formation of two grabens (wide rift), as illustrated in Figure 1.11.

Figure 1.11: Comparison of rift geometries for a) slow, and b) fast extension rates. Low rate extension induces the formation of a single, asymmetric graben. In contrast, higher rate extension leads to the formation of two grabens, one asymmetric and one near-symmetric. After Michon & Merle [2003].

The relation between slow extension and narrow rifts suggested by Brun & Beslier [1996] and Michon & Merle [2003] conflicts with the numerical modelling of Bassi [1995]. As Bassi [1995] considers the temperature dependence of rheology and the YSE in her model she finds that slow extension is likely to result in wide rifts. This is because runaway thinning is less likely to occur in slowly extended lithosphere that can thermally equilibrate during rifting.

The relationship between rheology, lithospheric strength, and thermal processes during rifting is clearly complex. The number of variables involved in continental extension and rifting are such that no model, as yet, can adequately incorporate all these variables. Indeed, few rift models exist which do not contradict the assumptions of other rift models, each of which can explain aspects of the same rift system.

1.3 Isostasy and Flexure

Deep margin drilling has revealed sedimentary deposits of shallow water (<200 m) origin at depths of many kilometres (e.g. Totterdell *et al.* [2000]). This provides clear evidence for major subsidence at rifted margins following breakup. Although sediment loading

and thermal relaxation contribute to the observed subsidence at margins, the isostatic compensation of crustal thinning at rifted margins provides a first order control on margin evolution. Each of the above rift models invokes local or regional isostatic compensation to explain rift margin subsidence. A brief history of the concept of isostasy and the salient differences between local and regional isostasy is given here.

Isostasy is the term used to describe a condition to which the Earth's crust and mantle tend, in the absence of disturbing forces [Watts, 2001]. That is, it describes a state of equilibrium between the Earth's crust and the underlying mantle. Due to the dynamic nature of surface Earth, the equilibrium state is constantly shifting; mountain chains are formed and eroded, river deltas grow, ice sheets wax and wane, and volcanoes form and disappear violently. The ideal isostatic state is disturbed by the dynamic and continuously changing mass distribution on surface Earth. Seismic and gravity data, however, suggest that the Earth's outermost layers generally adjust to these disturbances [Watts, 2001].

Early models of isostasy were proposed by Pratt [1855] and Airy [1855] to explain a discrepancy of over $5''$ between survey positions determined using triangulation and astronomical methods in the Himalayas, northern India. Pratt [1855] applied a model based on dividing the Himalayan range into columns of varying densities above a compensation depth at which lithostatic pressure was equal (Figure 1.12a). Pratt's theory failed to correctly predict the observed difference between the astronomical and geodetic calculations.

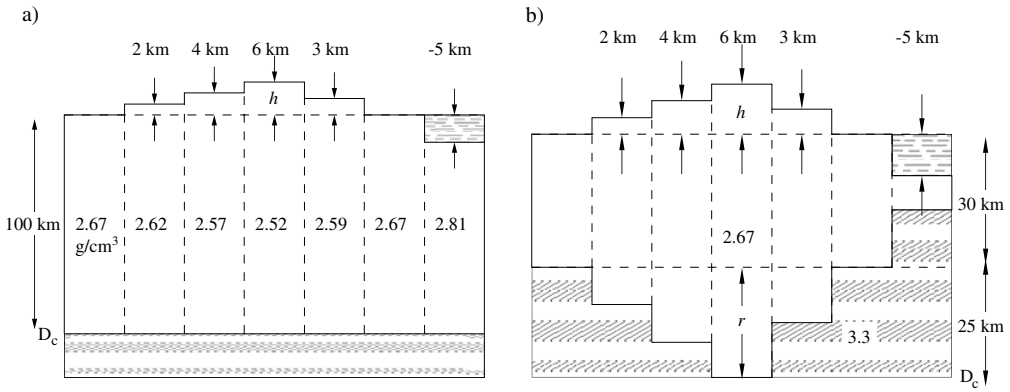

Figure 1.12: a) Pratt's model of isostatic compensation. Topography, h, is supported by density contrasts, above a depth of compensation, D_c, relative to standard density crust. b) The Airy model of isostasy. Topography of height h is supported by a crustal *root*, r, of lower density relative to mantle density. Figure modified from Stewart [1998].

Following the failure of Pratt's theory of isostasy to correctly predict the difference between the astronomical and geodetic calculations in northern India, Airy [1855] pre-

sented an alternative model. Airy demonstrated that if the excess mass of the mountains was supported at depth by a mass deficiency then the discrepancy could be accounted for (Figure 1.12b). He proposed that similarly to icebergs in the ocean, a mountain range was compensated at depth by a root of a relatively lower density than the mantle (or *"lava"* as Airy referred to it) displaced by the root. Which was the more appropriate and applicable model of isostatic compensation remained the subject of ongoing debate for over a century [Watts, 2001].

The Pratt and Airy models of compensation are based on contrasting assumptions, however, they are similar in that they consider compensation to occur on a purely *local* scale. That is, the compensation of topography occurs directly below the topography. If it is assumed that the lithosphere has a finite strength or rigidity, then the compensation of topography or anomalous mass can occur over a greater area as it is supported by the lateral strength of the plate. This is the basic premise of *regional* compensation. The broader wavelength, but smaller peak amplitude, of regional compensation relative to local compensation is illustrated in Figure 1.13.

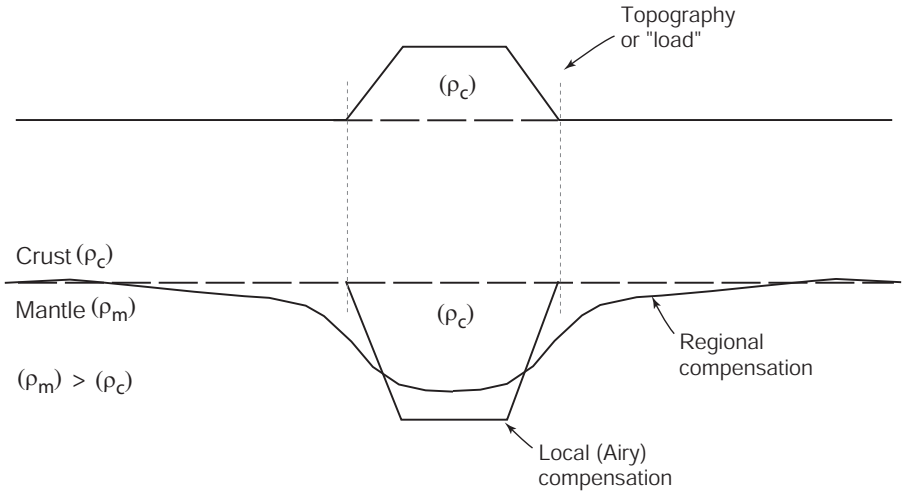

Figure 1.13: Schematic illustration of local and regional modes of compensation. ρ_c = crustal density, ρ_m = mantle density.

The notion of rigid lithospheric plates of finite strength was introduced in a series of papers by J. Barrell [1914] (as summarised by Watts [2001]). Vening Meinesz [1932] and many subsequent workers further developed this concept to incorporate an *elastic lithosphere*, capable of supporting stresses over geological time-scales (>1 My). In this model, the lithosphere is considered as a thin elastic sheet or plate overlying a fluid substratum. The deflection of such a plate is described by the general equation,

$$D\frac{d^4w}{dx^4} + (\rho_m - \rho_{infill})wg = 0 \qquad (1.1)$$

where ρ_m and ρ_{infill} are the densities of the mantle and infilling material, respectively, w is the deflection, and g is the acceleration due to gravity. D is the flexural rigidity of the plate, defined as,

$$D = \frac{ET_e^3}{12(1-\nu^2)} \tag{1.2}$$

where E is Young's modulus, ν is Poisson's ratio, and T_e is the *effective or equivalent elastic thickness*.

Equations 1.1 and 1.2 relate flexural rigidity to deflections of the lithosphere associated with loading forces. They also introduce the concept of effective or equivalent elastic thickness, herein referred to as elastic thickness, T_e. T_e does not represent the physical thickness of the rigid crust or lithosphere, rather it provides an equivalent elastic beam or plate thickness required to produce the observed or predicted deflection of the lithosphere to a given load. Although T_e relates to *rigidity*, it is often interpreted in terms of flexural *strength*, (e.g. Karner & Watts [1982]).

Estimates of T_e have been made in diverse geologic and tectonic environments, such as, the oceans (e.g. [Watts, 1978]), foreland basins (e.g. [Karner & Watts, 1983]), passive margins (e.g. [Stewart *et al.*, 2000]), trenches (e.g. [Parsons & Molnar, 1976]), and cratonic terranes (e.g. [Forsyth, 1985]). Estimates are typically based on spectral methods, such as admittance and coherence, or using forward modelling to fit observed crustal flexure and gravity anomalies.

The T_e evolution of oceanic lithosphere follows a predictable pattern controlled primarily by plate and load age (Figure 1.14), as demonstrated by Watts [1978]. Watts [1978] showed that T_e in the Pacific Ocean conformed to the depth of the $450 \pm 150°C$ isotherm. It is evident that this correspondence applies to most of the worlds ocean basins (see Watts [2001] for summary and references), and the range of T_e estimates for oceanic crust fall almost entirely within ~2-50 km.

In contrast, T_e estimates from continental interiors are far more varied [Burov & Diament, 1995; Watts, 2001]. T_e values ranging from 7.5-110 km have been recovered using various methods (see Watts [2001] for summary and references). A compilation of continental T_e estimates derived from foreland basin and glacial lake studies (Figure 1.15) shows no systematic correlation between T_e and either age of the load or thermal age of the lithosphere. Many of the larger continental T_e estimates have been determined using the spectral coherence of Bouguer gravity anomalies with topography. The validity of these high estimates has been questioned in recent years.

McKenzie & Fairhead [1997], Maggi *et al.* [2000] and McKenzie [2003] challenge the validity of T_e estimates that exceed the seismogenic thickness (T_s) of ~10-40 km. They claim that the strength of continents resides in the seismogenic layer within the crust

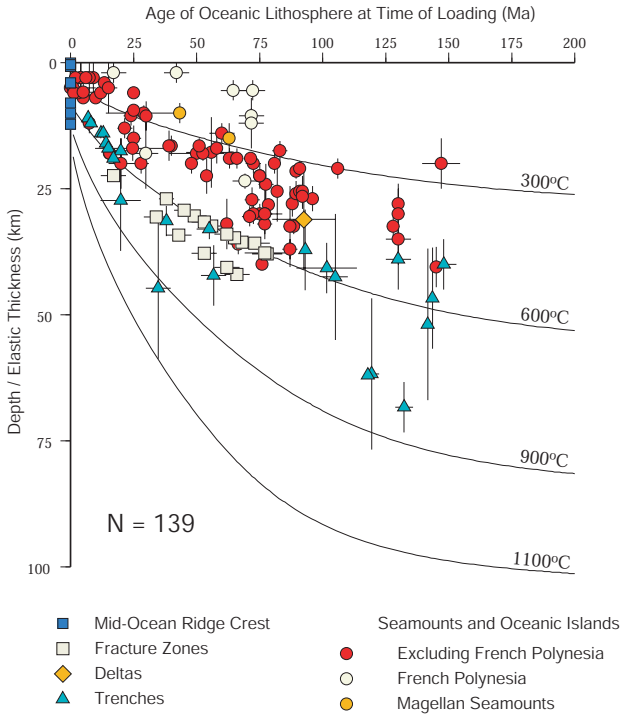

Figure 1.14: Plot of T_e against the age of oceanic lithosphere at the time of loading. T_e estimates are clustered between the depth to the 300 and 600°C isotherms. After Watts [2001].

and that continental mantle lithosphere is relatively weak. Perez-Gussinye *et al.* [2004] demonstrate that the application of spectral methods without adjustment for multi-tapering effects (associated with the size of the window used in spectral analyses) results in downward biased T_e recovery. McKenzie & Fairhead [1997] and McKenzie [2003] fail

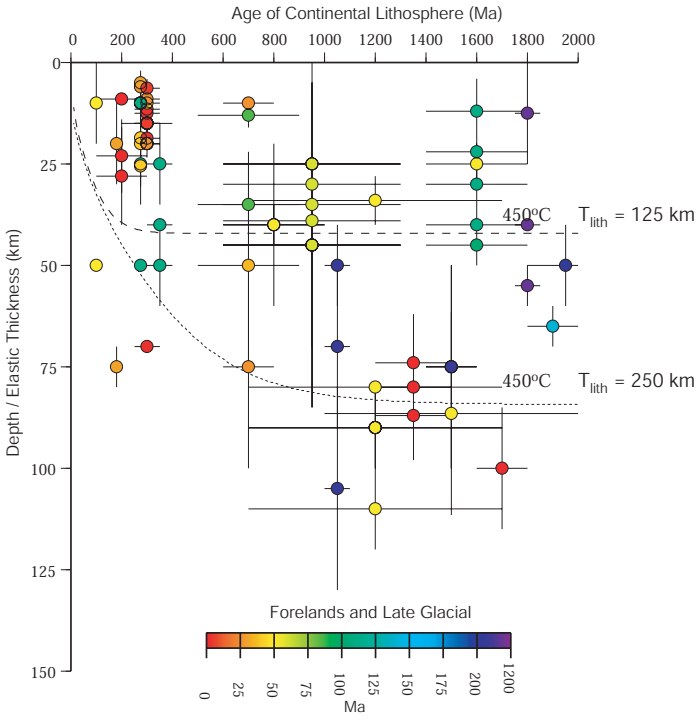

Figure 1.15: Plot of T_e against age of continental lithosphere at the time of loading. No correlation is evident as was the case for oceanic lithosphere and the scatter of estimates is much greater. After Watts [2001].

to make this adjustment in their studies that indicate $T_e \leq T_s$.

Watts & Burov [2003] find that that $T_e >> T_s$ in cratons, many convergent zones and some rifts. Most rifted margins, however, are characterised by low T_e, which is attributed to extensional faulting, thinning, and heating during intra-cratonic rifting, and post-rift sediment loading. Observation of flexure at seamounts has been widely used to constrain T_e estimates in oceanic lithosphere. Estimates of T_e in continental lithosphere are more commonly based on flexure at foreland basins or spectral studies (admittance and coherence). However, at rift margins where large sediment accumulations are common, spectral techniques are not applicable, and gravity modelling is typically used to provide constraints on T_e structure.

1.4 Gravity Modelling

Gravity anomalies can provide important insights into lithospheric structure. The density contrast across the *Moho* makes an important contribution to the gravity field at rifted margins. As models of compensation are intrinsically linked to the *Moho*, isostasy is important in understanding the gravity field at rifted margins. Additionally, analyses of observed and modelled gravity anomalies can elucidate the mode of isostatic compensation, and therefore the thermo-mechanical properties of the lithosphere, at rifted margins.

The initial development of a rift basin (i.e. prior to sediment deposition) causes two main contributions to the free air gravity field. The first is the negative anomaly associated with the replacement of crust by water/air. If the basin is in Airy isostatic equilibrium, the thinned crust and water filled basin are compensated directly beneath the basin by a mantle shallowing (Figure 1.16). The gravitational effect of this mantle shallowing is a positive anomaly. Away from the basin edge, the free air anomalies approach zero. However, over the basin edge a positive-negative couple, often referred to as the *"edge effect"*, occurs (observed edge effect anomalies over a number of rift margins are illustrated in Figure 1.3). The form of the anomaly is a function of the slightly lower magnitude and greater wavelength of the mantle compensation anomaly. This occurs as gravitational force is inversely proportional to the square of the distance to an anomalous mass.

The free air gravity edge effect anomaly at continental margins is one of the most distinctive features of the marine gravity field. It has been modelled and interpreted using various models of isostatic compensation. Worzel [1968] demonstrated the impact on the edge effect anomaly of moving the COB landward or seaward of the shelf break using an Airy isostatic model. Talwani & Eldholm [1973] also attempted to use Airy

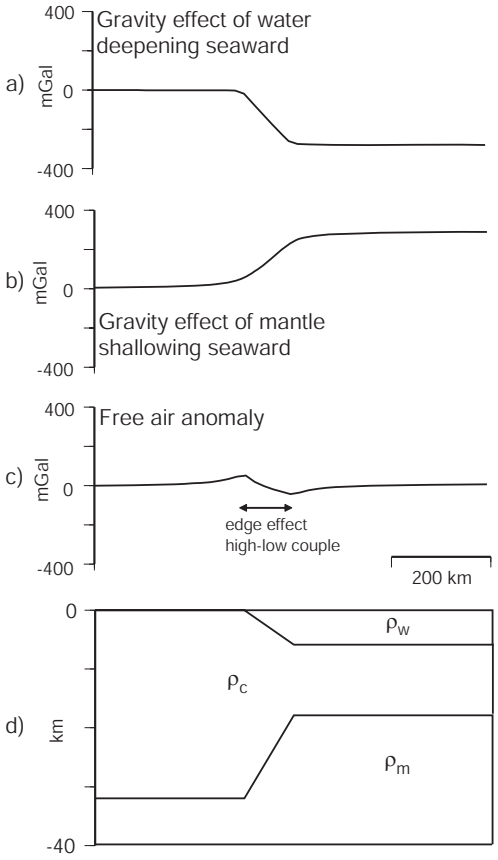

Figure 1.16: Illustration of the contributions of topography and its compensation to the free-air and Bouguer gravity anomalies at a rifted margin. Where $\rho_m = 3300$, $\rho_c = 2800$, and $\rho_w = 1030\,kg/m^{-3}$.

isostatic anomalies to assist in the identification of the continent-ocean transition (COT). This work was extended by Rabinowitz & LaBrecque [1977] to compensate the overlying sediments using an Airy model. They showed that the outer high isostatic anomaly, recognised by Talwani & Eldholm [1973], was not reduced by considering the sediments to be locally compensated. Both Talwani & Eldholm [1973] and Rabinowitz & LaBrecque [1977] interpreted this outer high anomaly to be associated with density differences within the crust and used it, along with other geological and geophysical features, as one criteria diagnostic of the COB.

Walcott [1972] and Cochran [1973], realising the potential importance of flexure at margins, employed the thin elastic plate model in gravity studies of the Mississippi and Amazon river deltas respectively. The results of these studies suggested an important role for flexure at rifted margins. Watts & Ryan [1976] also recognised that sediments at rifted margins represent a surface load that likely cause flexure of the crust and lithosphere. Accordingly, they surmised that an Airy model of isostasy, that assumes local rather than regional compensation, may not be appropriate in such environments.

In an attempt to quantify the effect of flexure on the edge-effect anomaly, Karner & Watts [1982] used spectral techniques (admittance) to estimate T_e in a rift margin

setting. They demonstrated that the outer high anomaly of Talwani & Eldholm [1973] could be explained by lithospheric flexure associated with sediment loading. As a result of this development, studies have been conducted, using seismic data where available to constrain sediment loading and crustal structure, to evaluate the spatial and temporal variation of T_e at rifted margins [Watts, 1988].

Watts & Marr [1995] present synthetic gravity models of *weak* ($T_e = 0$) and *strong* ($T_e = 25$) rifted margins to relate observed differences in edge effect anomalies to flexural strength. They illustrated that the edge effect anomaly is strongly dependent on the mode of compensation, local or flexural, of the sediment load. Watts & Marr [1995] show that a *"double"* edge effect anomaly is diagnostic of a weak margin, whereas a *"single"* edge effect anomaly indicates a strong margin.

Watts [1988] introduced a process-oriented approach to gravity modelling at rifted margins that accounts for the individual processes (i.e. crustal thinning, sedimentation, magmatic underplating) that contribute to the final form of the edge effect anomaly. This technique uses the observed gravity anomaly to constrain flexural rigidity of the lithosphere across rifted margins. Process-oriented modelling was also successfully applied in three-dimensions offshore west Africa, allowing segmentation of lithospheric strength to be inferred [Watts & Stewart, 1998].

Variation in T_e across a rifted margin is likely due to the formative processes involved in rift margin evolution. Continental margins comprise, by definition, continental, rifted continental, and oceanic lithosphere. The rheological and YSE changes associated with rifting of continental crust and the magmatic activity associated with seafloor spreading are likely to affect the long-term rigidity of the rifted continental crust. Therefore, T_e boundaries may represent fundamental changes in the underlying lithosphere and assist in identifying the COB.

Process oriented modelling differs fundamentally from object oriented modelling; a term used here to refer to gravity models that comprise bodies of varying (within a reasonable range as determined from empirical petrophysical measurements) density and geometry as required to model observed data. Object-oriented models provide constraints on the present-day mass distribution only, whereas process-oriented modelling allows the gravity contributions of geological processes to be investigated along with the mass distribution. Typically it is possible to achieve much closer fits to observed data (i.e. lower root mean square (RMS)) with object oriented models. However, due to the large number of bodies and parameters often utilised they are very sensitive to user input.

1.5 Thesis Outline

This thesis primarily analyses and integrates the results of three recently acquired, independent, geophysical datasets on the Wilkes Land margin of East Antarctica. These data were acquired by Geoscience Australia (GA) during two surveys (GA-228 and GA-229) carried out in the Austral summers of 2000-01 and 2001-02. The major geographic and morphologic features of the southeast Indian Ocean and East Antarctica are illustrated in Figure 1.17. The Wilkes Land sector of the East Antarctic margin extends from approximately 100-140°E and is conjugate to the southern margin of Australia. The conjugate margin pair is separated by an uninterrupted ocean basin, however, two oceans (the Southern Ocean[1] and the southeast Indian Ocean) are defined between Australia and Antarctica.

Interpretation and modelling, where appropriate, of seismic reflection, magnetic anomaly, and gravity anomaly data from surveys GA-228 and GA-229, and from previous surveys for which data is available, has been carried out to help understand the evolution of this rifted margin. Previous constraints on the crustal structure, age, seismic stratigraphy, subsidence history and thermomechanical evolution of the Wilkes Land margin are limited relative to the margins of all other continents. The primary reason for this lack of knowledge has been the absence of deep-penetrating, regional seismic reflection data. Sectors of the Wilkes Land margin had remained entirely unsurveyed prior to surveys GA-228 and GA-229.

As this thesis incorporates the analysis, or modelling and interpretation, of three independent datasets, it is split into three main chapters. The structure is as follows:

- Chapter 2 reviews the tectonic, geological and geophysical setting of the Antarctic continent, with specific focus on the Wilkes Land margin. A review of previous work is also included.

- Chapter 3 summarises the acquisition and processing of seismic reflection data offshore Wilkes Land.

- Chapter 4 describes the seismic stratigraphy of the Wilkes Land margin sedimentary section and the crustal structure as determined from seismic reflection data. The first sediment isopach for the Wilkes Land margin illustrates a major sedimentary basin off west Wilkes Land. Due to the almost total ice sheet cover of Antarctica, the marine sedimentary record of the Antarctic margin provides the only accessible record of palaeoevolution of the continental mass. The post-rift stratigraphy is of particular importance as it records the climatic transition from temperate to polar-glacial. A frag-

[1] In 2000, the International Hydrographic Organization delimited the Southern Ocean, it is defined as the ocean that surrounds Antarctica and extends to 60°S

ment of continental crust (?microcontinent), located at abyssal depths, that extends over 450 km from the shelf break is also identified off east Wilkes Land.

- Chapter 5 outlines the seafloor spreading magnetic modelling undertaken to constrain the timing of breakup between Antarctica and Australia. Modelling of magnetic anomaly data in relation to the geomagnetic time scale is crucial in further constraining the timing of breakup and the location of the COB. Problems associated with identifying the oldest true isochron are discussed critically.

- Chapter 6 contains the theoretical background of the backstripping process and process oriented gravity modelling. Modelling is conducted to create isostatic anomaly profiles and grids, and to constrain flexural rigidity variation across and along the margin. Primarily modelling is two-dimensional, using seismic reflection data to constrain model geometry, however, three-dimensional modelling is also completed. Gravity modelling herein provides the first insights into the lithospheric rigidity or strength of this rifted margin.

- Chapter 7 contains analyses and discussion of crustal structure and subsidence. Object oriented gravity modelling (forward and inverse) is completed to constrain the properties of bodies associated with isostatic anomalies calculated in the previous chapter. Object oriented magnetic modelling is also carried out to provide further insight to the nature of linear magnetic anomalies in the COT. A comparison with the conjugate southern Australian margin is also undertaken.

- Chapter 8 concludes the primary findings of this thesis and outlines ideas for future work.

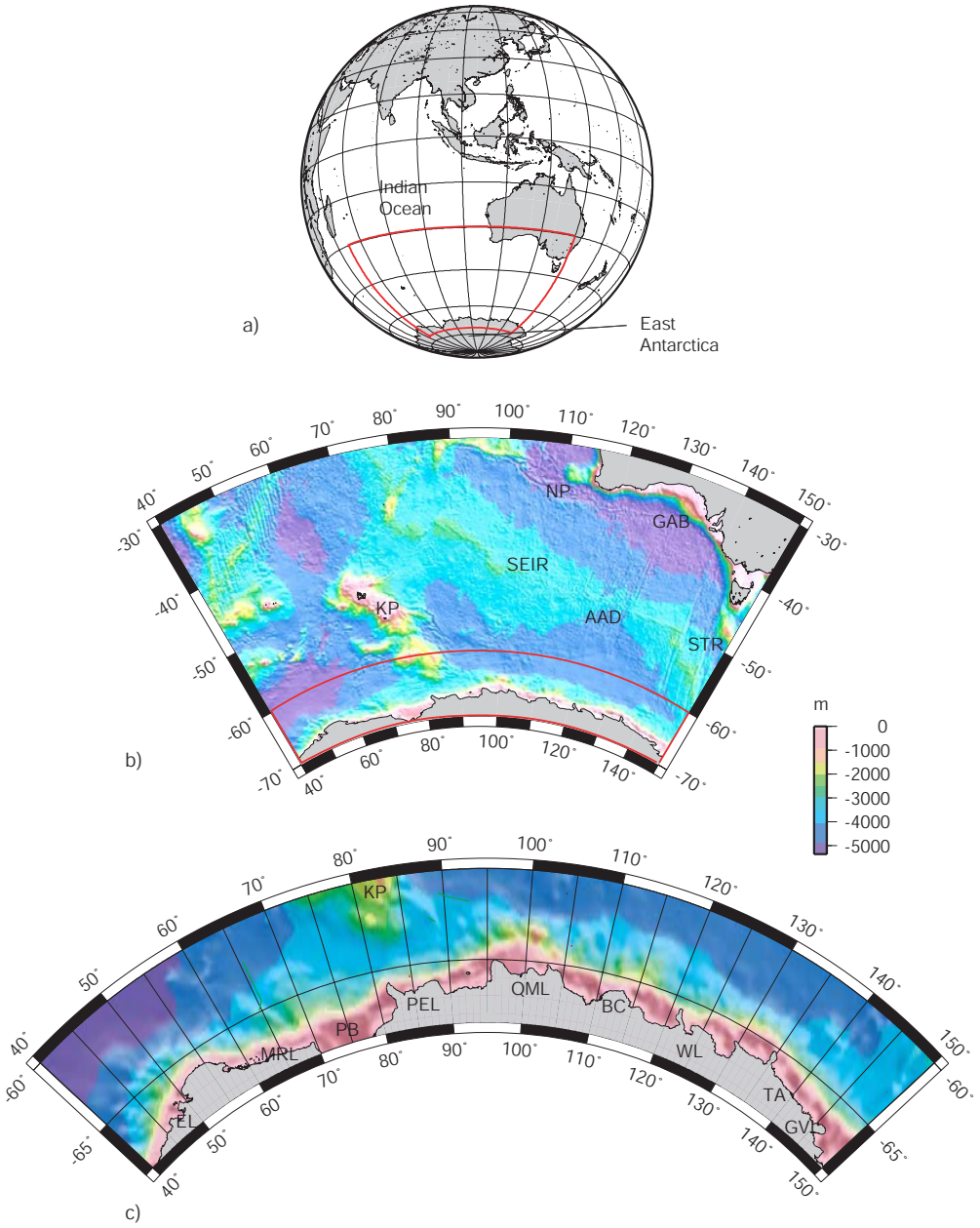

Figure 1.17: a) Location map of East Antarctica in a global context. b) Bathymetry map of the southeast Indian Ocean, the southern Australian and East Antarctic margins, and important morphological/geographical features. AAD = Australian-Antarctic Discordance, GAB = Great Australian Bight, KP = Kerguelen Plateau, NP = Naturaliste Plateau, SEIR = Southeast Indian Ridge, STR = South Tasman Rise. c) The Wilkes Land sector of East Antarctica is conjugate to the southern Australian margin. EL = Enderby Land, MRL = Mac.Robertson Land, PB = Prydz Bay, QML = Queen Mary Land, PEL = Princess Elizabeth Land, BC = Budd Coast, WL = Wilkes Land, TA = Terre Adélie, GV = George V Land. Bathymetry from Smith & Sandwell [1994].

Chapter 2

Geological and Geophysical Setting

2.1 Introduction

This chapter reviews the current state of knowledge relating to the tectonic history, geology and geophysics of Antarctica. The fragmentation and dispersal of the supercontinent Gondwana is reviewed in order to place Antarctica, in particular the Wilkes Land margin of East Antarctica, in a regional context

Due to the isolation and climate of Antarctica, and also the lack of commercial exploration and exploitation, the Antarctic continent remains a frontier realm of geology, of which very little is known. The Antarctic continent is more than 98% ice covered, and consequently the knowledge of the subglacial geology is extremely limited.

2.2 Gondwana and the Southern Continents

The notion of a continuous continental mass that once connected South America, Africa and India, was first suggested by in the late nineteenth century by Neumayr and Blanford (see Du Toit [1937] for references and historical discussion). The concept was further developed by Suess [1904], who conferred the name *"Gondwána-Land"*[1] to the prehistoric landmass. Du Toit [1937] observed that during the early twentieth century the former existence of Gondwana was to many *"...as nebulous as the mythical island 'Atlantis'"*.

The first comprehensive account of the geological basis for the existence of Gondwana was given by Du Toit [1937]. His primary aim was to provide scientific rigour to the concept of *continental drift*, as proposed by Wegener [1912] and Wegener [1915], which remained incomprehensible to most scientists of the time. Du Toit [1937] provided

[1] After *"...the ancient Gondwána flora common to all its parts"* [Suess, 1904]; although it is commonly thought that the name originates from a region of eastern India where some of the geology of the ancient continent was determined. However, as *Gondwana* translates to *"Land of the Gonds"*, Gondwana-Land would translate to "Land of the Gonds Land", which is nonsensical. Accordingly, the name Gondwana is more commonly used today, this convention is followed herein.

detailed descriptions of similarities in the faunal assemblages, sedimentology, and geological structures of the southern continents, which once comprised Gondwana, as evidence of continental drift theory. The reconstructions of Gondwana provided by Du Toit [1937], Figure 2.1, have been only slightly revised in over 65 years.

Figure 2.1: Gondwanan reconstruction of Du Toit [1937] at three intervals during the Mesozoic, 1. Early Jurassic, 2. *earliest* Cretaceous, and 3. *latest* Cretaceous.

Gondwana once formed the southern terrane of the Palaeozoic Supercontinent Pangaea, the northern terrane being Laurasia. These geologically and tectonically distinct terranes rifted apart to become isolated supercontinents during the Jurassic (e.g. Evans [2003]). Gondwana was by far the larger of the two supercontinents, with an estimated area of over 100×10^6 km^2 [Parrish, 1990]. Due to its size, the influence of the continent on global current and climate patterns would have been great. The relative positions of Gondwana and the south pole would have influenced the onset and duration of southern hemisphere glaciation, and consequently global sea level [Parrish, 1990].

The present day Antarctic continent formed the core of the Gondwanan Supercontinent, *"around which, with wonderful correspondences in outline, the remaining 'puzzle-pieces' of Gondwana can with remarkable precision be fitted"* [Du Toit, 1937]. Before the onset of breakup in the Middle Jurassic, Figure 2.2, Gondwana comprised continental crust that is now divided into a number of distinct plates. The major present-day plates that formed part of Gondwana are Antarctica, Australia, Africa, India and South America.

Figure 2.2: Gondwana tight fit reconstruction and breakup model, after Fitzgerald [2002], continent and microplate positions from Lawver *et al.* [1992] and Lawver *et al.* [1998]. AP = Antarctic Peninsula, TI - Thurston Island, MBL = Marie Byrd Land, CR = Chatham Rise, CP = Campbell Plateau, SNZ = southern New Zealand, NNZ = northern New Zealand, LHR = Lord Howe Rise, WS = Weddell Sea.

A number of major tectonic events shaped the present day continents, that once formed Gondwana, before the final breakup of the Supercontinent. The first of these is recognised as the onset of regional extension in the Early Permian, which produced a large rift and associated basins on what is now the east coast of Africa. Continuing extension led to the onset of breakup at approximately 150 Ma [Rabinowitz & LaBreque, 1979] when western Gondwana, comprising Africa and South America, separated from eastern Gondwana, comprising India, Antarctica, Australia and New Zealand [Smith & Hallam, 1970; Lawver & Scotese, 1987].

From the onset of Permian extension, through to Gondwanan breakup, large scale magmatic activity resulted in the widespread intrusion and eruption of intermediate to mafic, tholeiitic magmas. This period of extended magmatic activity is represented in southern Africa by the Karoo basalts (220-130 Ma) [Cox *et al.*, 1967], in Antarctica by the Ferrar dolerites and the Kirkpatrick basalt (180-160 Ma) [Tingey, 1991b], and in southeastern Australia by the Tasmanian dolerites (180-160 Ma) [Green *et al.*, 1978].

The separation of Greater India from East Antarctica, at ∼128 Ma, continued the west to east *unzipping* of Gondwana [Mishra *et al.*, 1999]. Following the separation of Greater India, all that remained of the former Supercontinent was the East Antarctic

terrane, the microcontinental blocks of West Antarctica and, the Australian and New Zealand terranes.

The Pacific margin of Gondwana was active during breakup, and subduction of the Phoenix Plate [Larson & Chase, 1972] continued throughout the Mesozoic. Subduction was occurring beneath the microcontinents and microplates of what are now New Zealand and West Antarctica, referred to here as Zealandia [Luyendyk, 1997] (Figure 2.2). At ~105 Ma, subduction was replaced by an extensional tectonic regime throughout Zealandia. This was followed about 20 My later by rifting and seafloor spreading between the Campbell Plateau and West Antarctica [Luyendyk, 1997]. The change in tectonic environment is most commonly attributed to subduction of the ridge crest (ridge capture), e.g. Larter & Barker [1989], or by capture of part of the subducted/subducting Phoenix Plate by the northward moving Pacific Plate (e.g. Luyendyk [1997]).

Whatever the cause, the change to an extensional rift regime in the West Antarctic region represented one of the final tectonic events that contributed to the piecewise fragmentation of Gondwana. The rifting of Australia and Antarctica represented the final development of extensional plate margins within Gondwana. Although the exact timing of this rift event has been equivocal for some decades, it appears certain that final separation and seafloor spreading commenced in the Late Cretaceous [Cande & Mutter, 1982; Tikku & Cande, 1999; Sayers *et al.*, 2001]. The oldest oceanic crustal age estimates from the Australia-Antarctic basin range from 83-95 Ma, however, final clearance of the Antarctic Plate and the South Tasman Rise occurred much later, ~35-29 Ma [Lawver & Gahagan, 2003; Cande & Stock, 2004].

Although the reconstruction of Gondwana is broadly well constrained (e.g. Smith & Hallam [1970], Lawver & Scotese [1987]), the exact locations of Madagascar with respect to Africa, the fit of Sri Lanka and India with East Antarctica, and the location of the Antarctic Peninsula with respect to South America have, at times, been equivocal [Lawver & Scotese, 1987]. However, advances in the identification of marine magnetic anomalies and the mapping of fracture zones in satellite altimeter derived bathymetry and gravity data have resolved most of these sources of controversy [Dalziel, 1992].

Reconstructions of Australia and Antarctica are, on a broad scale, also well constrained [Grindley & Davey, 1982]. However, a number of uncertainties remain regarding the reconstruction of the eastern Australia-Antarctic Basin (AAB) in the region of the South Tasman Rise (STR) (Figure 2.3). Although it is accepted that the STR comprises two distinct continental fragments, the East STR and the West STR, their kinematic evolution is uncertain. Due to the relatively small size of the STR it has either been ignored in some Gondwanan reconstructions, or is left in the same position relative to Tasmania as today [Royer & Rollet, 1997]. Irrespective, the STR causes a degree of

overlap with the Ross Sea Shelf or Victoria Land (e.g. Weissel *et al.* [1977], Grindley & Davey [1982]).

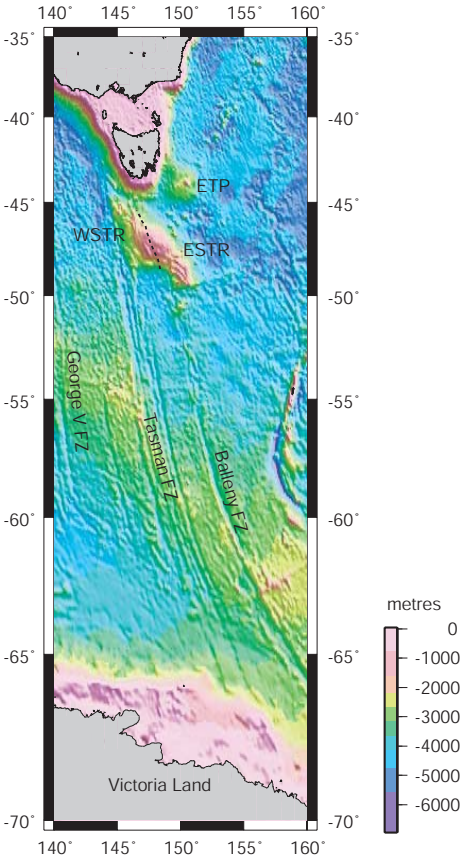

Figure 2.3: Eastern Australia-Antarctic Basin (AAB) bathymetry. Tight fit reconstructions consistently result in overlap of the East South Tasman Rise (ESTR) and West South Tasman Rise (WSTR), and Victoria Land, Antarctica. The Balleny fracture zone (FZ) marks the continuation of the East Antarctica-West Antarctica continent-continent boundary. ETP = East Tasman Plateau.

Royer & Rollet [1997] suggest a reconstruction in which the East and West STR have distinct kinematic histories in an attempt to solve the overlap problems. They suggest that the West STR was initially attached to Antarctica and underwent severe wrench deformation as the Antarctic plate moved southward relative to the Australian plate. Whereas, they suggest that the East STR rifted from southern Tasmania and the East Tasman Plateau. However, Gaina *et al.* [1998] suggest that if the likely Cainozoic extension in the western Ross Sea is considered, there is insufficient space for the STR in the total fit reconstructions of Royer & Rollet [1997]. Revised reconstructions of Tikku & Cande [1999] encounter the same overlap problems (Figure 2.4). Possible explanations for the consistent overlap problems suggested by Tikku & Cande [1999] include:

1. That the previously recognised oldest seafloor spreading anomalies are not isochrons.
2. The rotation poles for the oldest isochrons are incorrect.
3. That, as yet unidentified, post 80 Ma, continental extension has occurred in the Bass Strait region of southeastern Australia or northern Victoria Land, Antarctica.

Figure 2.4: Reconstructions of Australia and Antarctica in the region of Tasmania and Victoria Land, Antarctica for isochrons 32y, 33o, 34y, and the quiet zone boundary (QZB) anomaly. Antarctic COB (solid black line) is from Eittreim [1994], and the Australian COB (outlined white line) is digitised from the satellite free air gravity grid by Tikku & Cande [1999]. Dotted and dashed lines are the Australian and Antarctic *"continental margins"*. Figure from Tikku & Cande [1999].

The solution to the continental overlap observed in plate reconstructions of the eastern AAB remains a *"tectonic puzzlement"* [Tikku & Cande, 1999]. The acquisition of further geophysical data is required to more adequately resolve the kinematic evolution of this region. The tectonic evolution of West Antarctica also remains somewhat equivocal. However, it is not investigated further here as it is of little relevance to the region of study for this thesis.

2.3 Timing of the Antarctic-Australia Breakup

Correctly dating the onset of seafloor spreading between Antarctica and Australia is of fundamental importance to understanding the geological evolution of this conjugate margin pair. However, the timing of separation between Australia and Antarctica has been highly equivocal for the last three decades. Breakup ages from 52 to 125 Ma have been argued by workers since the early 1970's.

The continental margins of Antarctica and Australia are currently separated by the approximately 3000 km-wide Southern Ocean and southeast Indian Ocean. The Southeast Indian Ridge (SEIR), which is located approximately half-way between the continents, trends east-west, at a latitude of ∼50°S, as far as 139°E. East of this longitude, the SEIR is offset to the southeast by a zone of transform faults to nearly 65°S [Veevers, 1987]. The AAB is the only region along the length of the SEIR in which there is a recognised magnetic sequence for the oldest period of seafloor spreading from the Late Cretaceous to the early Tertiary [Cande & Mutter, 1982]. Although the anomaly sequence is complete it is far from ideal; the anomalies are generally poorly formed and exhibit significant variations in their form along strike. There is also a relative paucity of data on the Antarctic margin, forcing interpretations to include unconstrained interpolations of significant magnitude between shiptrack data.

Weissel & Hayes [1972] suggested that Australia-Antarctic separation occurred in the Early Eocene (52 Ma), based on the identification of anomaly 22 as the oldest seafloor spreading anomaly on the southern margin of Australia. A major revision of this breakup age was proposed by Cande & Mutter [1982] following their reinterpretation of southern Australian margin seafloor spreading anomalies. Cande & Mutter [1982] concluded that anomalies 19-22 of Weissel & Hayes [1972] could be better modelled as anomalies 20-34. Accordingly, they revised the age of separation from ∼53 Ma to 86-110 Ma during the long Cretaceous normal polarity epoch.

More recently, Sayers *et al.* [2001] have interpreted seafloor spreading onset at anomaly 33o time (∼79 Ma), some 15 My younger than the 95 Ma age accepted for much of the previous two decades. A full discussion of previous work on magnetic modelling in the Southern Ocean and the evolution of the revisions made to the breakup age of Antarctica and Australia is given in Chapter 3.

2.4 East Antarctica and West Antarctica: Surface, Crust, and Lithosphere

One of the broadest observations of Antarctica is the obvious division between East Antarctica and West Antarctica, Figure 2.5. The geological basis for this division was documented by some of the earliest workers in the area [Tingey, 1991b; Bentley, 1991].

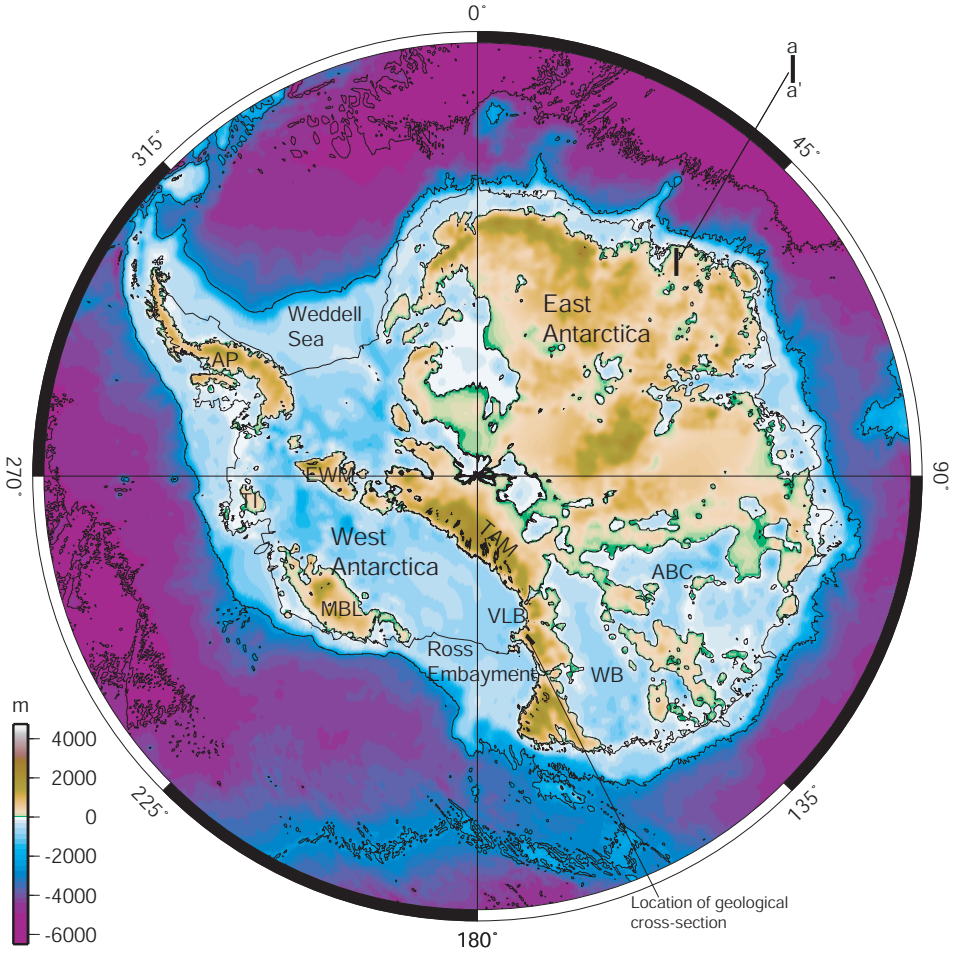

Figure 2.5: Topography of Antarctica from the BEDMAP project [Lythe *et al.*, 2000]. The Transantarctic Mountains (TAM) form the physiographic divide between East Antarctica and West Antarctica. Profile a-a' is illustrated in Figure 2.6. WB = Wilkes Basin, ABC = Aurora Basin Complex.

The boundary between East and West Antarctica is very abrupt, as seen from both the topographical divide at the Transantarctic Mountain (TAM) front, and from geophysical evidence that indicates a rapid change in crustal and lithospheric thickness [Bentley, 1991]. Seismic refraction experiments in East Antarctica indicate a depth to the *Moho* of ~38-40 km inland, Figure 2.6, decreasing to ~30 km at the coast [Kogan, 1972; Ikami

et al., 1983]. Whereas, the depth the *Moho* in West Antarctica is generally <30 km (e.g. Bentley [1983]). Gravity modelling (e.g. Groushinsky & Sazhina [1982]) also indicates greater crustal thickness in East Antarctica.

Figure 2.6: An example of a deep seismic sounding profile from East Antarctica, as located in Figure 2.5, after Ikami *et al.* [1983].

Seismic tomography reveals a marked difference in lithospheric properties between East Antarctica and West Antarctica. Figure 2.7 illustrates that East Antarctica is characterised by faster relative (to PREM, [Dziewonski & Anderson, 1981]) S-wave velocities, at a depth of ~150 km, than West Antarctica. Broadly, this represents a greater depth of cooler, continental mantle lithosphere beneath East Antarctica relative to West Antarctica. The TAM front, the physiographic divide between East Antarctica and West Antarctica, and the steepest S-wave velocity perturbation gradient correlate extremely closely.

The different geological framework of the two terranes is also apparent in the subglacial topography, Figure 2.5. East Antarctic subglacial topography is generally above sea level, the East Antarctic flank of the TAM extends for hundreds of kilometres under the East Antarctic Ice Sheet (EAIS). In contrast, the elevation drop on the West Antarctic flank of the TAM is much steeper.

East Antarctica can be divided into two main sectors, the Indian Ocean (0-90°) and Australian (90-180°) sectors, on the basis of subglacial topography. In the Indian Ocean quadrant, bedrock lies mostly above, and in extensive mountainous regions, far above, sea level. In contrast, the Australian quadrant comprises two extensive subglacial and sub-sea-level basins, the Wilkes Basin and Aurora Basin Complex (ABC), separated by rugged highlands.

Distinctive, mesa style landforms (i.e. flat-topped areas of elevated topography),

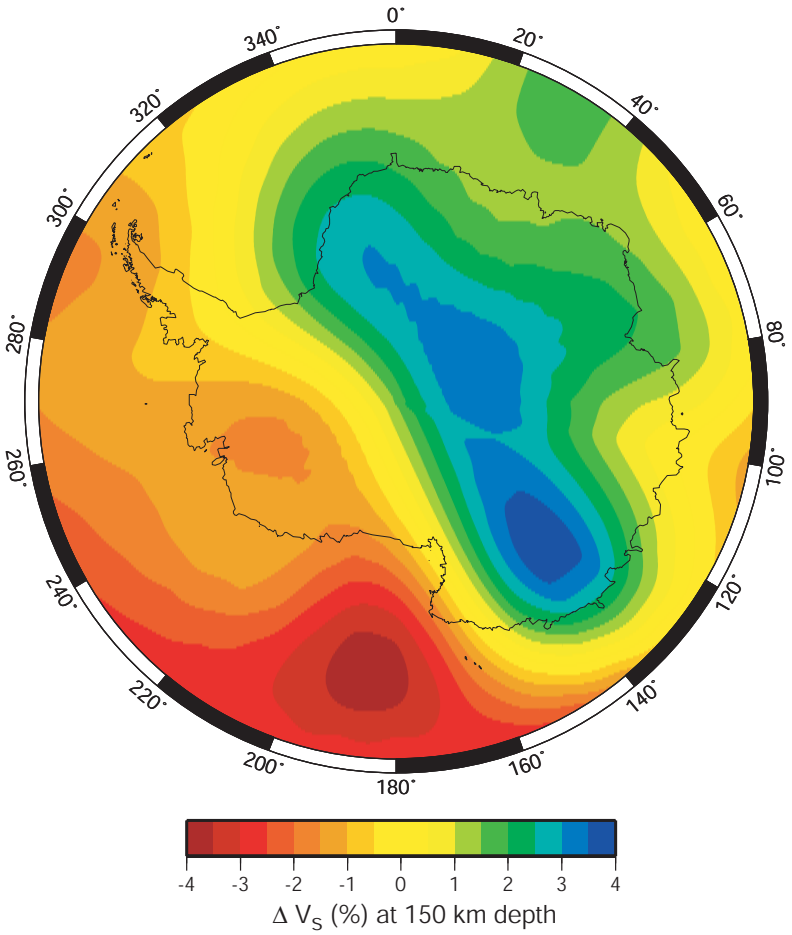

Figure 2.7: Perturbations in S-wave velocity, relative to PREM [Dziewonski & Anderson, 1981], from the S2ORTS model of Ritsema *et al.* [1999], at a depth of 150 km. The transition from fast to slow S-wave velocities correlates to the TAM front, and the boundary between East Antarctica and West Antarctica. Figure generated by K. Chambers.

identified in radio echo-sounding data, beneath the ice sheet covering Wilkes Land have been correlated with similar features observed in Queen Maud Range and in northern Victoria Land [Steed, 1980]. The Karoo Group of southern Africa is also characterised by similar landforms. Steed [1980] infers that these features are formed from eroded Beacon Supergroup sediments, and provide another link between the Gondwanan continents.

The West Antarctic subglacial topography contrasts strikingly with that of East Antarctica. A great topographic depression starts at the Ross Sea, and flanks the West Antarctic TAM front for almost their entire length. Regions of this depression lie more than 1000 m below sea level. The permanent ice sheet prevents West Antarctica from becoming an archipelago of continental islands.

Antarctic topography is very unusual relative to other continents. No other continent

exhibits a markedly bi-modal hypsometric curve [Cogley, 1984]. The bi-modal distribution of continent-wide bedrock elevation is not accounted for by isostatic compensation of the estimated ice load differences in each region. Cogley [1984] estimated deglaciated bedrock elevation modes of -450 m and 950 m (relative to mean sea level) for West Antarctica and East Antarctica respectively.

Differences in topographic, crustal, and lithospheric character and palaeomagnetic history are observed between East Antarctica and West Antarctica. This supports the notion of a continent-continent boundary at the TAM.

2.5 The Transantarctic Mountains

The Transantarctic Mountains (TAM) are located along the continent-continent boundary between West Antarctica and East Antarctica (Figure 2.5). They form the physiographic, geological, and geophysical divide between these two distinct continental terranes. The TAM provide most of the best outcrops in Antarctica, and are therefore important in understanding the geological evolution of the whole continent. The TAM form a 3500 km-long belt of elevated topography, locally reaching elevations of over 4500 m. Although the major period of uplift occurred in the Cainozoic, the structural backbone of the TAM comprises Proterozoic rocks, deformed and metamorphosed by the 500 Ma Ross Orogen [Elliot, 1975; Tingey, 1991b].

Following the uplift and granitoid intrusions associated with the Ross Orogen, Silurian to Early Devonian erosion formed the Kukri Peneplain [Gunn & Warren, 1962]. The Devonian to Jurassic, ~3 km thick, Beacon Supergroup overlies the Kukri Peneplain [Quilty, 1986; Barrett, 1991]. The Beacon Supergroup has been extensively intruded by Ferrar Group dolerites and basalts during the Jurassic [Tingey, 1991b]. A summary geological cross section of the TAM is shown in Figure 2.8.

Figure 2.8: Geological cross section of the TAM showing the geological relationship between the crystalline, metamorphic basement, the Beacon Supergroup, and the Ferrar Supergroup. The Kukri Peneplain is an angular unconformity that separates basement from the Beacon Supergroup, from ten Brink *et al.* [1997]. See Figure 2.5 for location.

The Kukri Peneplain is extensively exposed throughout the TAM, and can be used as an indicator of the pre-uplift topography of the region because the overlying Beacon Supergroup remains relatively undeformed [Quilty, 1986]. The Peneplain is interpreted to have been at depths of ∼2.5-3.5 km at the end of Beacon Supergroup deposition, to accommodate the shallow marine and fluvial deposits [Barrett, 1991]. It is now observed at elevations of over 4000 m, which gives an indication of the amount of uplift parts of the TAM have undergone. Smith & Drewry [1984] estimate an average uplift rate of 90 m/My for the last 45 My, based on geological data. Apatite fission track data indicates similar rates, 100 m/My for the last 50 My (e.g. Fitzgerald *et al.* [1986]).

The exact mechanism of uplift of the TAM continues to be debated. Various thermal and isostatic models have sought to constrain the mechanisms for the rapid and large magnitude uplift. Fitzgerald *et al.* [1986] suggested that underplating and low-angle simple shear were the primary mechanisms. Heat conduction, isostatic forces, and erosion were cited by Stern & ten Brink [1989] and ten Brink *et al.* [1997], and extensional necking of the lithosphere was proposed by van der Beek *et al.* [1995]. Due to difficulties in acquiring regional geophysical and geochemical data at the TAM, it is difficult to objectively assess the merits of each model. However, factors common to the various models, such as; a thermal gradient between the thin West Antarctic lithosphere and the thick East Antarctic lithosphere, a flexural component associated with the free-edge of the East Antarctic plate and the load of the EAIS, and upward forcing associated with valley incision within the TAM; provide a basis for explaining much of the uplift.

The TAM are characterised by a lack of folding or thrust faulting, and are generally described as a series of simple, asymmetric fault-blocks [Fitzgerald, 2002]. The TAM are interpreted to represent rift-shoulder uplifts supported by flexure of the strong East Antarctic lithosphere, that have formed in response to the divergent nature of the boundary between East and West Antarctica [Stern & ten Brink, 1989].

Rift flank uplifts are typically no more than 1000-2000 m high and exhibit half wavelengths (i.e. the distance from the axis of maximum uplift to the topographic minimum formed behind the uplift) on the order of 150 km (e.g. Steckler [1985]). In this regard, the TAM appear to be an extreme case of rift shoulder mountains as they have experienced uplift of over 4500 m and have a half wavelength of 400-500 km [Stern & ten Brink, 1989]. The significance of the TAM is also attested to by the fact that the lateral continuity of the chain is approximately 3000 km, similar to mountain ranges such as the Andes and Himalayas.

Adjacent to the West Antarctic flank of the TAM is a vast, submerged region of extended and rifted continental crust, the Ross Embayment. Ross Sea rift basins run parallel to the TAM and contain up to 14 km of sediments, over crust thinned to less

than 20 km, e.g. Melhuish *et al.* [1995] and Cooper *et al.* [1987]. Parallel to the East Antarctic flank of the TAM, but set back some 400-500 km, is the subglacial Wilkes Basin, a major basin of contentious origin and nature that will be discussed in detail later in this chapter.

2.6 West Antarctica: Tectonics and Geology

Palaeomagnetic and (limited) geological data indicate that West Antarctica comprises a number of distinct crustal blocks or lithospheric microplates. The exact number and kinematic histories of these microplates is uncertain, (e.g. Dalziel & Elliot [1982], Storey *et al.* [1998]). The Ellsworth-Whitmore Mountains crustal block (EWM), Antarctic Peninsula, Thurston Island, and Marie Byrd Land are generally accepted as the major West Antarctic microplates (Figure 2.5). In addition to these four main microplates, a number of smaller blocks are also utilised in reconstructions (see Fitzgerald [2002] for summary).

The Ross Embayment, incorporating the Ross Sea and Ross Ice Shelf, is interpreted as an area of active extension, the West Antarctic Rift System (WARS), between East Antarctica and West Antarctica [Dalziel & Elliot, 1982; Cooper *et al.*, 1987]. Except for the area beneath the Ross Sea, the WARS is not constrained in detail. A number of asymmetric grabens are imaged beneath the Ross Sea, which are interleaved by basement highs (e.g. Cooper *et al.* [1987]). The sedimentary basins within these grabens have been formed by extension since the Mid-Jurassic, however, the main phase of extension in the WARS occurred in the Late Cretaceous (e.g. Lawver & Gahagan [2003]). Post-early Oligocene extension is only inferred within a narrow zone of the Victoria Land Basin [Cooper *et al.*, 1987].

Estimates of the total amount of extension between East and West Antarctica vary widely, from 400-1800 km. The methods of estimating the extension are also varied, and include plate reconstructions (e.g. Stock & Molnar [1987]), one-layer stretching models (e.g. Bentley [1991] and Lawver & Scotese [1987]), and palaeomagnetic studies (e.g. Storey *et al.* [1998]). Palaeomagnetic studies predict greater amounts of extension relative to the other methods. Although the mechanism of extension is also poorly constrained, Fitzgerald & Baldwin [1997] suggest that extension has been primarily accommodated by low-angle, detachment faulting.

Outcrop in West Antarctica consists almost entirely of Mesozoic and Cainozoic rocks. Although sedimentary and metamorphic outcrops do occur, volcanic and plutonic rocks are far more common and comprise the majority of outcrop. The Cainozoic magmatism evident in West Antarctica is coeval with East Antarctica-West Antarctica rifting, and the main uplift phase of the TAM. The Mary Byrd Land province is the locus of more recent

volcanism. It is roughly in the centre of a belt of mid- to late-Cainozoic alkaline volcanoes that extend along the continental margin from the tip of the Antarctic Peninsula to northeast Victoria Land.

Continental basement, where observed, in West Antarctica comprises variably metamorphosed Precambrian rocks. Gneiss and schist country rock is heavily intruded by granites, felsic pegmatites, and mafic dykes. Overlying the basement are Precambrian to Mesozoic sequences of greywacke, shale, conglomerate and chert, that is variably deformed and metamorphosed. Detailed summaries of West Antarctic geology are provided by Tingey [1991b], Barker *et al.* [1991], and LeMasurier & Rex [1991].

2.7 East Antarctica: Tectonics and Geology

Geological mapping in East Antarctica is limited to sporadic outcrops along the coast, in interior highland areas, and the TAM. Mapping of such outcrop indicates a basement complex of mainly early Precambrian age, comprising primarily high-grade metamorphic gneisses and schists along with charnockitic rocks [Tingey, 1991b]. This basement underlies almost all of East Antarctica and constitutes the East Antarctic Shield. Overlying the basement sequence are Precambrian to Cambrian sedimentary rocks and some volcanic rocks which represent typically flat-lying platform deposits [Quilty, 1986].

The best exposed rock sequences are reported in the TAM. The relatively flat-lying sedimentary beds of the Beacon Supergroup, overlying the Kukri Peneplain, comprise Devonian marine rocks disconformably underlying extensive exposures of non-marine Permian and Triassic rocks [Barrett, 1991]. Sedimentation through the Permian and Triassic resulted in this 2700-3500 m sequence of sandstone, interbedded with coal and glacial sediments, in intracratonic or foreland basins parallel to the palaeo-Pacific margin [Quilty, 1986].

Extensive, plume-generated magmatism is interpreted to have accompanied the initial Gondwana breakup (e.g. Cox [1988]). Large-scale, within-plate mafic and felsic magmatic provinces in many Gondwanan continents, including Antarctica, were formed by active plume processes [Fitzgerald, 2002]. Plume magmatism is represented in Antarctica by the Ferrar Group tholeiites (Kirkpatrick Basalt and Ferrar Dolerite), which formed at approximately 180 Ma [Tingey, 1991a]. However, the Ferrar province reflects melting of more depleted lithospheric source mantle than other coeval rocks found elsewhere in Gondwana [Elliot, 1992].

The Ferrar Group forms the Antarctic segment of a long linear belt of a mafic magmatic province that extends from Tasmania and southeast Australia, to southern Africa. Peak eruption rates within this belt are inferred between 175±18 Ma [Green *et al.*, 1978]

and 182±2 Ma [Hooper *et al.*, 1993]. This short eruption time is similar to other continental flood basalt provinces [Fitzgerald, 2002]. The linear distribution of the magmatism is not compatible with classic circular plume models, and so Cox [1988] proposed a hot-line rather than a hot-spot.

[Storey & Kyle, 1999] suggest that a Gondwana 'megaplume' existed in the Weddell Sea region as a result of a spreading centre triple junction. In this model, production of magma batches associated with plume-lithosphere interaction, migrated along zones of crustal weakness forming the linear magmatic provinces. White & McKenzie [1989] suggest that the present day location of the plume is at Bouvet Island.

2.8 Antarctic Margin Physiography

Except for the Antarctic peninsula, the margins of Antarctica are exclusively passive rift margins. The margins of Antarctica likely followed a typical pattern of thermal subsidence and sediment deposition following breakup. However, they now exhibit physiographic characteristics unlike most rift margins. The morphological development of the Antarctic continental margin has been largely controlled by glacial and glacimarine processes since the development of permanent polar ice at ∼34 Ma (e.g. Exon *et al.* [2002] and Cooper & O'Brien [in press]).

Bathymetry compilations of the ocean encircling Antarctic and the marginal seas (i.e. Weddell Sea and Ross Sea) are poorly constrained relative to the margins of all other continents as a relatively limited amount of shiptrack data is available. Additionally, bathymetry derived from satellite altimetry data (e.g. Smith & Sandwell [1994]) is less reliable than at lower latitudes, due to the presence of grounded- and sea-ice on the Antarctic margins (e.g. McAdoo & Laxon [1997]).

Two compilations of bathymetry data are available for the Southern Ocean (i.e. for latitudes south of 60°S). These are the BEDMAP [Lythe *et al.*, 2000] and GEBCO 1-minute [IOC *et al.*, 2003] grids. The BEDMAP grid is a 5×5 km grid for the continent and seabed south of 60°S, which is based on a compilation of open-file shiptrack data supplemented by satellite derived bathymetry from [Smith & Sandwell, 1994]. The GEBCO data is based on shiptrack data only and has a nominal resolution of 1-minute, however, in some areas the data density is not great enough to warrant this resolution. The two grids differ locally as demonstrated for the Wilkes Land margin later in this chapter. Gross morphologic trends and characteristics can be equally well interpreted from either grid.

The Antarctic continental shelf is characterised by a number of distinct features that contrast with continental margin environments in more temperate climates. These

features include rugged topography, great depth, highly varied and commonly broad width, and its glacial setting [Anderson, 1991]. Anderson [1991] estimates an average shelf depth of ∼500 m. Near coastal, narrow troughs that exceed 1000 m depths have been observed in echo-sounding data since the earliest marine surveys and are common and characteristic of a number of regions of the Antarctic margin, (e.g. Escutia *et al.* [2000]). Some cross-shelf troughs extend seaward from the termination of major present-day glaciers and/or ice tongues, however, not all can be genetically related to the present-day glaciomorphology of the adjacent margin.

In many areas around East Antarctica, the continental shelf slopes towards the continent. This does not occur on continental margins in more temperate latitudes. Isostatic downwarping or flexure caused by the ice sheet load contributes to this, and also to the great depth of the shelf [ten Brink *et al.*, 1995]. However, glacial erosion is the primary control on the geometry, depth and rugged topography of the Antarctic continental margin. Direct evidence of glacial erosion is seen in almost all seismic profiles acquired on the margin [Anderson, 1991].

2.9 Glacial History

The sudden, widespread glaciation of Antarctica and the associated shift toward colder temperatures during the Cainozoic represents one of the most fundamental reorganisations of the global climate system recognised in the geologic record [De Conto & Pollard, 2003]. Timing the onset of Cainozoic glaciation, which has been the subject of debate since the earliest surveys of Antarctica, is important for a number of reasons. Widespread ice sheet development lowered the pre-glacial continental shelf through a combination of glacial erosion, and flexural downwarping associated with ice-loading, profoundly influencing the establishment of the present glacial maritime setting and oceanographic circulation. On a more global scale the event also triggered massive changes in global climate patterns [Kennett, 1977].

The original, and widely accepted, model of glacial onset invoked the thermal isolation of Antarctica as the catalyst for regional glaciation within Antarctica, and the onset of a global ice-house climate [Kennett, 1977]. This thermal isolation is interpreted as a function of deep seaways surrounding Antarctica. Continental palaeomagnetic data (e.g. Lawver & Gahagan [2003]) and seafloor spreading anomaly modelling (e.g. Royer & Rollet [1997]) support the notion of deepening seaways at ∼29-34 Ma between Tasmania and East Antarctica, and South America and the Antarctic Peninsula.

More recently it has been recognised that the opening of circum-Antarctic seaways is only one of a number of contributing factors to the evolution of the Cainozoic climate

(e.g. Zachos *et al.* [2001]). Coupled global climate-dynamical ice sheet modelling by De Conto & Pollard [2003] attempted to quantitatively constrain the varying contributions to the inception and growth of the East Antarctic Ice Sheet. De Conto & Pollard [2003] use climate-ice sheet simulations to investigate the effects of declining atmospheric CO_2, compared to those of the tectonic opening of Southern Ocean gateways, and timing of mountain uplift in the Antarctic interior. Their results contrast with the established paradigm of thermal isolation as a catalyst for regional glaciation, and indicate that instead, declining CO_2 may have been the primary causative mechanism. Their models of glacial expansion also do not suggest a strong feedback from the inclusion or exclusion of highland areas.

Whether a primary cause of glaciation or not, geological evidence suggests major environmental changes were associated with the opening of deep seaways around Antarctica. The two constrictions on a circum-Antarctic ocean, from Gondwanan breakup until the Late Eocene, were the southern tip of South America, and the Tasmania-South Tasman Rise system. The timing of the Tasman Gateway[2] and Drake Passage openings are considered, therefore, to have influenced the major shifts in climate patterns.

The most recent attempt to date the onset of glaciation and describe the palaeoenvironment at the time of, and following, the Tasman Gateway opening were made on Leg 189 of the Ocean Drilling Program (ODP) [Exon *et al.*, 2002]. Exon *et al.* [2002] identify a time of massive environmental change during the Late Eocene, 37-33.5 Ma. During this interval, fast seafloor spreading [Weissel & Hayes, 1972; Cande & Mutter, 1982] was moving Australia northward and the Tasmanian land bridge and its broad shelves had started to subside more rapidly.

A consequence of the deepening of the Tasmanian land bridge was that the warm shallow currents of the Pacific no longer reached the Antarctic margin. The effect of this was that cool shallow currents could penetrate from the previously isolated Australo-Antarctic Gulf (AAG) through the Tasman Gateway (Figure 2.9). The changes interpreted from well data during this interval are significant: from warm to cool climate; from poorly ventilated basins to well ventilated open sea; from dark siliciclastic to light pelagic, carbonate deposition; and from organic-rich to organic-poor sedimentation [Exon *et al.*, 2002].

Data from ODP Leg 189 indicate an abrupt change from the early Oligocene. Exon *et al.* [2002] suggest that warm tropical currents were completely cut off from some parts of the Antarctic margin by the developing ACC from this time. This likely precipitated the formation of highland glaciers, which formed the earliest components of the ice sheet

[2]Tasman Gateway describes the seaway that formed between the microcontinental blocks around the South Tasman Rise and northern Victoria Land, Antarctica.

Figure 2.9: Development of a circum-Antarctic ocean from 34-31 Ma. The northward motion of Australia allows the cool currents from the Australo-Antarctic Gulf (AAG) to penetrate the opening Tasman Gateway and isolate the Pacific margin of Antarctica from the warmer currents of the Pacific Ocean. The opening of the Drake Passage, between South America (SAM) and the Antarctic Peninsula, allows the Antarctic Circum-Polar Current (ACC) to develop. EANT = East Antarctica, AUS = Australia, NZ = New Zealand, KP = Kerguelen Plateau, BR = Broken Ridge, WS = Weddell Sea, RS = Ross Sea. Figure from Lawver & Gahagan [2003].

covering Antarctica today.

The timing and rapid onset of glaciation, extending beyond isolated highland areas, near the Eocene-Oligocene boundary (∼34 Ma), is also well constrained by ODP data from ODP Leg 188, in Prydz Bay. Palynological analyses indicate a humid and cool-cold climate persisted in the Prydz Bay region to the Late Eocene [Cooper & O'Brien, in press]. The earliest lithologic evidence of nearby highland glaciation is seen in late Eocene-age grain textures in massive sand units [Strand *et al.*, 2003]. The earliest evidence

of glacimarine erosion of the continental shelf are mid-Miocene deposits of reworked, Eocene-age, shelf environment foraminifera, encountered during drilling on the Prydz Bay continental rise [Cooper & O'Brien, in press]. The glacimarine reworking of shelf strata indicate that the ice sheet had grounded on sections of the East Antarctic continental shelf by the Mid-Miocene.

Early stages of ice sheet advance likely occurred under much less severe climatic conditions than exist at present. The cool-temperate conditions that prevailed throughout the early Tertiary, likely altered to temperate-glacial for a period before the polar-glacial environment observed today became stable. Temperate glacial environments are characterised by large sediment flux (e.g. Powell [1984]), in contrast to polar-glacial settings where sedimentation is significantly reduced (e.g. Hampton *et al.* [1987]). Polar-glaciers are typically characterised by low basal velocities and a freezing of the land surface [Eittreim *et al.*, 1995]. ODP results from Prydz Bay show a seven-fold reduction in sedimentation rates in the late Miocene (∼9 Ma), relative to peak sedimentation rates in the early Miocene, from 70 m/My to 10 m/My [Cooper & O'Brien, in press]. This reduction is interpreted to indicate close to peak glacial conditions being reached, however, as the well was located on the lower continental slope this is somewhat speculative.

Growth and development of the continental ice sheet probably lowered sea level enough to expose sections of the continental shelf to erosion by fringing elements of the ice sheet. Conceivably, this early ice sheet ablated by melting rather than iceberg calving [Anderson, 1991], and wet-based sliding would have been the dominant erosion mechanism. The combined effects of significant erosion and meltwater stream development emanating from glacier termini delivered large quantities of terrigenous sediment to the sea primarily in glacial deltaic deposits.

There is compelling evidence of subglacial till deposits on the continental shelf of a number of areas of the Antarctic margin [Anderson, 1991; Eittreim *et al.*, 1995]. This indicates that the Antarctic ice sheet grounded on the continental shelves of both West Antarctica and East Antarctica on one or more occasions since the Miocene. However, the exact timing of the glacial event(s) that led to the deposition of tills on the continental shelf is poorly constrained [Anderson, 1991]. Although near shore deposition continues today, surface geological processes have been relatively limited in the late Quaternary. The lack of any outcrops of Cainozoic sediments are an indication of this.

Estimates of present day ice thickness, primarily from airborne radar data, have been compiled by the BEDMAP project [Lythe *et al.*, 2000], Figure 2.10. These data illustrate that the regions of greatest ice thickness occur in East Antarctica, which comprises ∼90% of the ice in Antarctica [Bamber *et al.*, 2000]. A maximum ice sheet thickness of ∼4500 m is observed in East Antarctica, which is covered by an average 2500 m of ice.

Figure 2.10: Ice thickness grid of Antarctica, BEDMAP project data [Lythe *et al.*, 2000]. Greatest ice thickness is observed in East Antarctica, where 90% of all Antarctic ice is contained in the East Antarctic Ice Sheet. Figure from D. Vaughan, British Antarctic Survey.

Although on a broad scale the basal velocity of the East Antarctic Ice Sheet (EAIS) is very low relative to temperate glaciers, studies of *balance velocities* provide an insight into the dynamic nature of the EAIS [Bamber *et al.*, 2000]. The balance velocity represents the depth-averaged velocity required at any point to maintain the ice sheet in a state of balance, given a specified distribution of net surface mass flux. Balance velocity is calculated from the surface slope (estimated from satellite radar altimetry and terrestrial data) and ice thickness (as calculated by the BEDMAP project [Lythe *et al.*, 2000]). It is assumed that flow is parallel to the local topographic gradient within the ice sheet. In broad terms, the surface slope controls the spatial pattern of balance velocities, which are scaled as a function of ice thickness and the surface mass balance [Bamber *et al.*, 2000].

Bamber *et al.* [2000] calculated balance velocities for the grounded part of the Antarctic Ice Sheet, Figure 2.11. Complex flow patterns are observed throughout the continent.

Channelised flow can be clearly identified in the balance velocity distribution, however, the velocities of many of these 'channels' are lower than the typical range of ice-stream velocities of 100-2000 m/yr [Bentley, 1987]. Although lower than typical ice-stream velocities, the channels exhibit higher velocities than the surrounding ice sheet, which is characterised by balance velocities of <30 m/yr. The distinction between the slow-moving interior ice sheet and fast-moving outlet glaciers and ice streams is not as clear as has been previously believed [Bamber *et al.*, 2000].

Figure 2.11: a) Balance velocity estimates for grounded parts of the Antarctica ice sheet. b) Balance velocities for the Lambert Glacier region showing features that feed the Amery Ice Shelf. c) Balance velocities in the region of the Totten Glacier. Figure from Bamber *et al.* [2000].

Two regions of East Antarctica are characterised by large, relatively fast-flowing outlet glacier systems that are fed by complex tributary systems. The largest of these is the Lambert Glacier-Amery Ice Shelf region. The second, the Totten glacier region, exhibits similar balance velocity characteristics. However, it does not encompass as broad a catchment area as the Lambert Glacier. The Totten Glacier terminus is located at and around a topographic high on the Budd Coast sector of the west Wilkes Land coast.

2.10 Onshore Geology and Geophysics: 'Australian Sector', East Antarctica

2.10.1 Geology

The eastern extremity of the Wilkes Land sector of East Antarctica is bounded by the TAM, which form an almost complete barrier between the EAIS and the Ross Embayment and Victoria Land. The Wilkes Land sector is, in general characterised by basin development not seen in other areas of East Antarctica. The Wilkes Land coast provides little outcrop. Rare onshore outcrops comprise largely Precambrian medium- to high-grade metasediments, metavolcanics, granulites and charnockite bodies [Tingey, 1991b].

The best rock exposures in the region are found in the TAM. The sequence of outcrop generally observed comprises Precambrian basement (Robertson Bay Group) overlain by the Beacon Supergroup, which typically dip shallowly (∼5°) to the west [Tingey, 1991b]. In the eastern extremes of Wilkes Land, unmetamorphosed sedimentary rock outcrops are relatively common (by East Antarctic standards). At Horn Bluff (∼150°E) a ∼300 m high cliff capped by Ferrar Group dolerites reveals a section of Beacon Group sediments [Mawson, 1940], and Precambrian granulite facies and charnockite bodies. The latter are common throughout the East Antarctic Shield [Tingey, 1991b]. The lateral extent of the Beacon Group sediments in Wilkes Land, and East Antarctica more generally is uncertain.

The Beacon Supergroup has been identified in a number of regions of Antarctica, including the Prince Charles Mountains, Queen Mary Land, and the Shackelton Range; indicating a regional depositional system. The Devonian to Triassic aged Beacon Supergroup was one of the key factors in the first Gondwanan reconstruction of Du Toit [1937] as it is sedimentologically and petrologically very similar to the formations of the Gondwana Basin of eastern India, the Santar Katarina Supergroup in South America and, the Karroo Supergroup in southern Africa.

Gondwana reconstructions place the Queen Mary Land, Wilkes Land and Terre

Adélie-George V Land margins against the southern margin of Australia[3]. On the Australian margin, the extents of the rift system are marked by the Naturaliste Plateau, to the west, and the South Tasman Rise (STR), to the east. The conjugate features on the Antarctic margin are the Bruce Rise, in the west, and northern Victoria Land, in the east. A number of major basins occur on the southern Australian margin, including the Bremer, Bight, Duntroon, Otway, and Sorell Basins; collectively referred to as the Southern Rift System (SRS), e.g. Stagg *et al.* [1999]. A large sediment apron is also observed off the central southern Australian margin, the Ceduna Terrace. Basins of comparable magnitude have not previously been recognised on the Wilkes Land margin, and no major sediment terraces are observed.

The central conjugate margin sector is interpreted to have resulted from early northwest-southeast extension, followed by almost entirely north-south extension [Willcox & Stagg, 1990]. Spreading histories to the east and west of the central sector are more complex. The Queen Mary Land sector of the Antarctic margin occupies a complex tectonic position, where Australia-Antarctica spreading has overprinted the earlier spreading pattern of India-Antarctica. It has also been influenced by plume related emplacement of the large igneous province to the northwest, the Kerguelen Plateau [Veevers *et al.*, 1991]. In contrast, east of Wilkes Land, i.e. Terre Adélie and George V Land, the margin developed in a left-lateral rift/wrench system, e.g. Willcox & Stagg [1990]. Large fracture zones and spreading ridge offsets occur around the southeast Australian and STR margin.

2.10.2 Inland Basins: Flexure or Extension?

Two major sub-glacial basins and a number of troughs are apparent in the Wilkes Land interior. Interleaved with the areas of depressed topography are regions of rugged highlands, and relatively flat plain areas close to mean sea level (MSL) (Figure 2.12).

The Wilkes Basin broadly parallels the East Antarctic flank of the TAM, it is covered by an ice sheet of average ∼3 km thickness, and a maximum observed thickness of over 4.5 km (Figure 2.10). The basin axis is oriented broadly north-south for over 1400 km, from the coast to a latitude of ∼82°S, decreasing in width from ∼600 km at the coast to <100 km inland. The basin (as defined by the base of the EAIS) reaches depths of >1000 m relative to MSL, is characterised by relatively low base of ice gradients, and shallows towards the coast. The coastal sector of the basin exhibits greater topographic variation, and comprises a number of highland areas that locally subdivide the basin.

The eastern limits of the Wilkes basin are constrained by the TAM, whereas the western extent, and to a lesser degree the northern extents, are relatively discontinuous

[3]The Wilkes Land sector, as the largest sector conjugate to the Australian margin, is also used more generally to describe all sectors once conjugate to the southern Australian margin

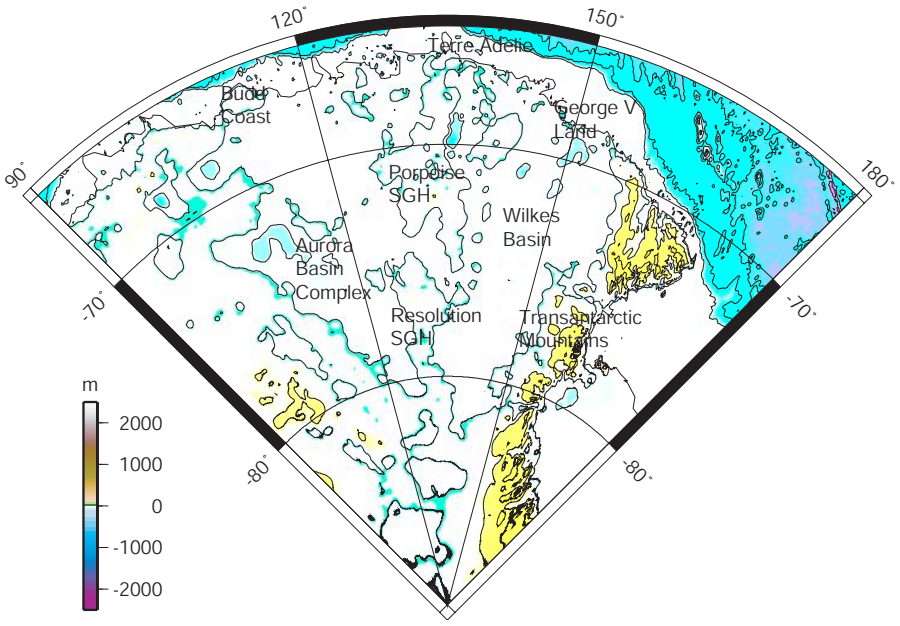

Figure 2.12: Sub-glacial bedrock topography of the 'Australian Sector' of East Antarctica. Two major basin systems dominate the topography, the Wilkes Basin and Aurora Basin Complex. SGH = sub-glacial highlands.

and interleave the bordering highlands at a number of locations. A broad correlation between increased topographical roughness (as measured by RMS deviation from mean elevation) and increased elevation is observed in the eastern sector of the basin, but this correlation decreases towards the west of the basin [Steed, 1980].

In the extreme west of the Wilkes Land interior is a secondary system of largely sub-MSL basins, the Aurora Basin Complex (ABC). The ABC, although of approximately similar proportions to the Wilkes Basin, forms a branching system of sub-basins that generally trend northwest towards the Wilkes Land coast. An even greater areal extent of >4 km thick ice is observed in the ABC relative to the Wilkes Basin. The ABC basins are generally deepest in the west, but two peripheral deeps are observed in the east. The ABC has a very sinuous outline, several sub-basins enter into bordering highland areas. Separating the Wilkes Basin and the ABC is a broadly north-south oriented region of rugged highlands, the Resolution and Porpoise Subglacial Highlands. These highlands are bounded both north and south by plains of low elevation. The southeastern end of the ABC forms a broad saddle with the southwestern limit of the Wilkes Basin, at the southern end of the Resolution Subglacial Highlands.

Geophysical data over the ABC is extremely limited. The Wilkes Basin has been the subject of much more extensive geophysical surveying. Geophysical methods have primarily been utilised to constrain the presence and thickness of sediments within the

Wilkes Basin, and to determine whether the basin has a flexural or rift-related origin.

Seismic refraction experiments in the northwest of the Wilkes Basin indicate seismic velocities typical of granitic bedrock (~5800 m/s), which was interpreted by Bentley [1974] to indicate that there were no sedimentary deposits of significant thickness within the Wilkes Basin. Radio echo-sounding data acquired subsequent to the refraction data illustrate that the refraction experiment was located on the flank of the basin, and therefore did not sample typical basin morphology [Steed, 1980].

Drewry [1976] interpreted radio echo-sounding data, and particularly the statistical correlation of elevation and topographical roughness to infer the presence, and map the extent, of basin sediments. Drewry [1976] cited the broad spatial correlation between the Wilkes Basin and "...strongly negative regional free-air and Bouguer anomalies..." as further evidence of sediment infill within the basin. He also suggested the lower frequency magnetic anomaly data over the basin, relative to surrounding highlands, was evidence of sediments covering the basin basement rock. Drewry [1976] suggested that up to 3 km of sediments underlie the Wilkes Basin.

Steed [1980] considered that the negative gravity anomaly over the Wilkes Basin may be a result of delayed isostatic compensation to the load of the ice sheet. Although it is possible that this could, in part, contribute to the anomaly, Steed [1980] considered it unlikely to fully explain an anomaly of the observed magnitude. The possibility of a mantle source for the anomaly, associated with the uplift of the TAM, was also suggested by Steed [1980].

Stern & ten Brink [1992] interpret the Wilkes Basin as the *"outer low"* associated with the flexural origin of the TAM. The flexural model proposed by Stern & ten Brink [1992] suggests the basin is a regional, flexural downwarp, associated with the uplift of the TAM. In this model, the Wilkes Basin is analogous, although in the opposite sense, to the flexural outer rise observed at the oceanic trenches of subduction zones. Gravity modelling carried out by Stern & ten Brink [1992], comparing the gravity profiles calculated assuming a strong crust (flexural model) and a weak crust (Airy model), supports a flexural origin for the Wilkes Basin. They also propose that peripheral uplift and broad, shallow hinterland basins may be common in other cratonic areas, particularly in areas once associated with the Gondawanan Supercontinent, for example the Murray Basin of southeast Australia and the Kalahari Basin of southern Africa.

A seismic reflection and gravity profile was completed over the Wilkes Basin in the austral summer of 1993-94 (East Antarctic Seismic Traverse 1993 - EAST93) ten Brink *et al.* [1997]. Data from this survey was used by ten Brink *et al.* [1997] to constrain models to support a flexural origin for the Wilkes Basin. They also interpret the data to indicate that:

1. Ferrar flood basalts extend for at least 100 km within the Wilkes Basin.

2. The Beacon Supergroup thins gradually within the Wilkes Basin, away from the TAM, indicating deposition occurred in a foreland basin.

3. There is no evidence of incomplete isostatic rebound due to melting of the East Antarctic ice sheet since the last glacial-maximum.

ten Brink *et al.* [1997] argue against the presence of Cainozoic sediment fill within the Wilkes Basin on the basis of gravity and magnetic modelling. They model the observed gravity anomaly by the flexure of the East Antarctic plate, using a broken plate model for the continent-continent boundary between West Antarctica and East Antarctica, and the presence of *"Beacon-type"* sediments thinning away from the TAM. Their model also requires thermal uplift associated with a double thickness crust for the East Antarctic craton (45 km), relative to West Antarctica, ice loading of East Antarctica, and erosional unloading within the TAM.

Ferraccioli *et al.* [2001] do not accord with the interpretation of a flexural origin for the Wilkes Basin. Using data acquired along the International Trans-Antarctic Scientific Expedition traverse (ITASE) during the austral summer of 1998-99, Ferraccioli *et al.* [2001] infer crustal thinning beneath the Wilkes Basin. They find that at 75°S the crust thins from 37 km below the TAM to 31±2 km beneath the Wilkes Basin. This interpretation is in direct contradiction of the flexural models of Stern & ten Brink [1992] and ten Brink *et al.* [1997], which predict crustal thickening beneath the basin. Ferraccioli *et al.* [2001] interpret the Wilkes Basin as having an extensional origin, on the basis of the thinned crust. This agrees with the earlier interpretation of Steed [1980]. They also interpret the adjacent Adventure Subglacial Trench as a narrow rift basin floored by thinned (25±5 km) crust with sediment infill of 6-14 km.

Gravity and magnetic models of Ferraccioli *et al.* [2001] incorporate Beacon-type sediments within the Wilkes Basin, and low density rift sediments in the Adventure Subglacial Trench. This is, again, in direct contrast to the models of ten Brink *et al.* [1997], which included no sediment within the Wilkes Basin. The EAST93 traverse modelled by ten Brink *et al.* [1997] did not go as far west as the ITASE line, and Ferraccioli *et al.* [2001] contend that this may explain why the rift gravity signature and the presence of a sedimentary gravity signature was not identified by ten Brink *et al.* [1997].

Ferraccioli *et al.* [2001] do not dispute the flexural support of the TAM by the East Antarctic craton, as proposed by Stern & ten Brink [1992]. If the TAM have a rift-flank origin, and the crust flooring the Wilkes Basin is thinned, as inferred by Ferraccioli *et al.* [2001], then likely the Wilkes Basin is flexurally induced (at least in part), and has also been subject to extensional rifting forces. The Wilkes Basin has been correlated, on the

basis of its geophysical characteristics (and location), with the Neoproterozoic Adelaide fold belt of Southern Australia (e.g. Oliver & Fanning [1997]).

The origin of the major basin systems of the Australian Sector of East Antarctica remain poorly understood. Further geophysical data, particularly seismic reflection and refraction data, are required to determine the genetic processes involved in their formation. With the current level of data, it is not even possible to conclusively determine the presence of Cainozoic (or older) sediments within the basins, much less their tectonic origin.

2.11 Wilkes Land Margin: Offshore Geology and Geophysics

The Wilkes Land region did not become a major research focus until the early 1980's when marine geophysical and geological surveys were conducted by the Institut Francais du Pétrol (IFP) [Wannesson *et al.*, 1985], the United States Geological Survey (USGS) [Eittreim & Smith, 1987], and the Japan National Oil Company (JNOC) (e.g. Tanahashi *et al.* [1987]). These surveys acquired multi-channel seismic and potential field data on the Wilkes margin in the early 1980's.

2.11.1 Physiography

The continental shelf of the East Antarctic margin is narrow relative to West Antarctica, averaging approximately 100 km in width between 60°E and 170°E. However, variations in width from 60-200 km are observed. The average width of the Wilkes Land continental shelf is ∼125 km. This sector of the margin is characterised by a steep upper slope, relative to other East Antarctic margin sectors, and a shelf-slope break that generally occurs at depths of 400-600 m. The most striking morphological features along the Wilkes Land margin are the dendritic, large-relief (>1000 m), cross-shelf trough systems. Eittreim *et al.* [1995] suggest that these canyons, which shoal from >1000 m on the inner shelf to ∼500 m on the outer shelf, are the paths of ice streams that extended across the shelf during times of glacial maxima. Sediment banks flanking these canyons are interpreted as areas where grounded ice was relatively immobile during the glacial maxima.

Bathymetry data from the BEDMAP [Lythe *et al.*, 2000] and GEBCO 1-minute [IOC *et al.*, 2003] compilations for the Wilkes Land margin are illustrated in Figure 2.13. The BEDMAP data has been resampled at a 1-minute resolution to allow a residual map of the difference in bathymetry between the two compilations to be calculated (Figure 2.13). Broadly, the two compilations are very similar, however, locally they differ by up to ∼1000 m. The greatest disparity in the compilations occurs at the shelf break in

west Wilkes Land. This is likely a function of resampling and subsequent gridding as BEDMAP data in this region is almost entirely extracted from Smith & Sandwell [1994].

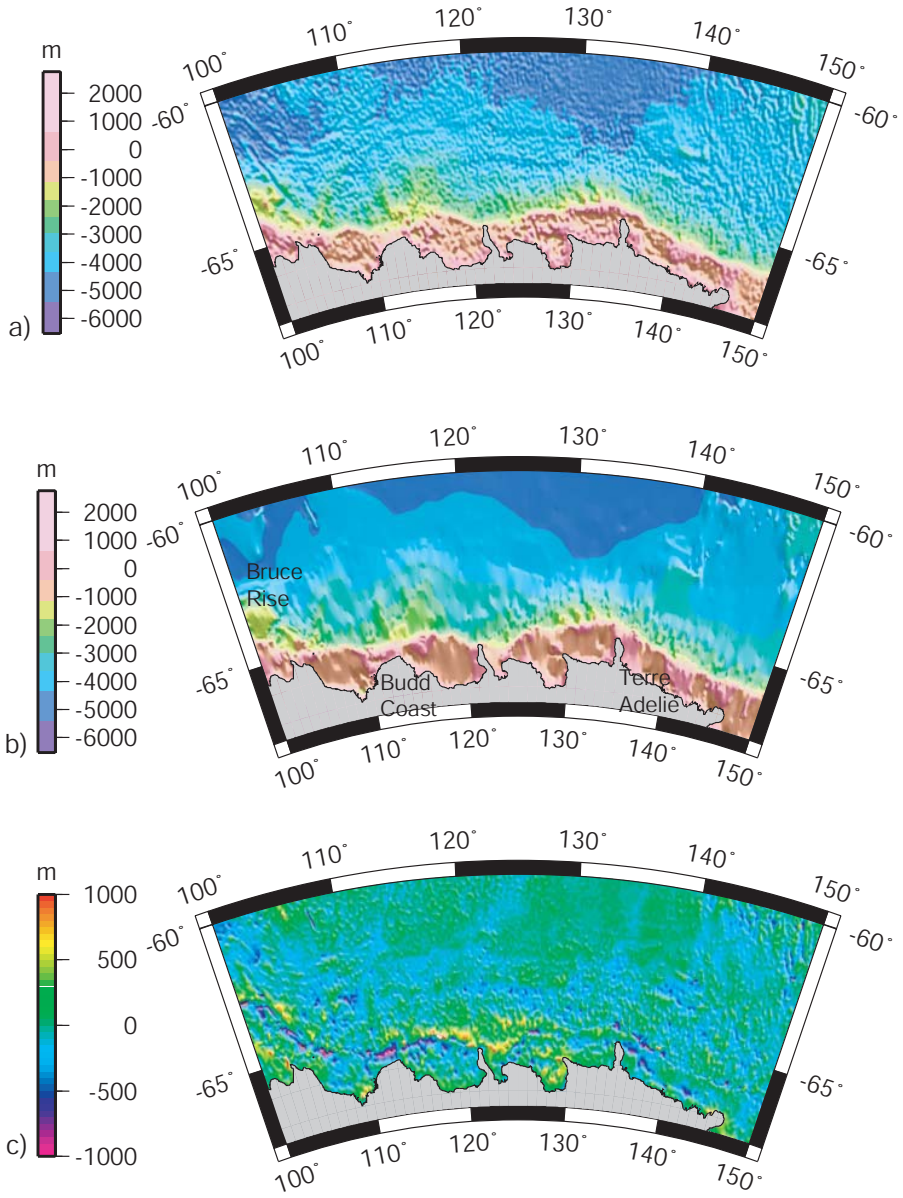

Figure 2.13: Bathymetry of the Wilkes Land margin from a) the BEDMAP project compilation, and b) the GEBCO 1-minute grid. c) The residual bathymetry (BEDMAP - GEBCO), locally the difference in the two grids reaches almost 1000 m at the shelf break off west Wilkes Land.

Seismic reflection data from the Wilkes Land continental shelf indicate significant erosion (100's m) (e.g. Eittreim *et al.* [1995]). The shelf is also over-deepened by ice sheet induced flexure of the crust (e.g. ten Brink *et al.* [1995]). In some areas the modern sea floor represents an unconformity associated with glacial erosion [Anderson,

1991]. Ice gouges are visible in sidescan sonar data to depths of over 500 m on the Wilkes Land margin, these gouges are represented by circular to subcircular depressions, 30-150 m in diameter [Barnes, 1987]. The presence of ice gouges indicate erosion and reworking of modern sediment by iceberg keels to depths of over 500 m. The upper sedimentary section has been glacially stripped on the inner shelf in some areas, exposing older strata and possibly acoustic basement [Eittreim *et al.*, 1995].

Bruce Rise, a marginal plateau at ∼100°E (Figure 2.14) marks the transition zone between the Greater India-Antarctic and Australia-Antarctic rifting events. This is the only marginal plateau recognised on the Australian sector of the East Antarctic margin. It acts as a physiographic barrier, separating the Wilkes Land margin from the Princess Elizabeth Trough and the Prydz Bay area. The plateau surface occurs at a depth of ∼1500 m, and the transition to abyssal depths at the seaward edge of the plateau is very rapid. Deep troughs also incise the continental rise to the east and west of the plateau. The Bruce Rise is interpreted to be conjugate to the Naturaliste Plateau off southwest Australia [Coleman *et al.*, 1982].

The continental shelf narrows massively at the Budd Coast, west Wilkes Land, and a clear shelf break can not be identified. In contrast, the continental shelf to the east and west of the Budd Coast is wide (>125 km), and is characterised by a distinct shelf break. The onshore Budd Coast comprises an elevated bedrock and ice surface, the Law Dome. The transition from the Law Dome to the continental slope is very rapid. This area is also the location of large-relief sediment ridges or banks, broadly oriented orthogonally to the margin. The ridges extend beyond the base of the continental slope, flanking deep troughs. Smaller magnitude, but similar geometry and character, sediment ridges occur off the Wilkes Land coast from 130-135°E, between the termini of the Dibble and Mertz Glaciers (Figure 2.14).

These networks of continental slope, cross-shelf troughs and flanking, channel-overbank deposits are interpreted by Escutia *et al.* [2000] to represent ice-sheet sourced turbidite fan systems. The Wilkes Land turbidite systems exhibit a number of systematic morphologic differences compared to most river-sourced fans, such as (after Escutia *et al.* [2000]:

1. Multiple large tributary channels across the upper and middle fan.

2. Channel relief several times greater (900 m) than typical relief (100-200 m) for channels on fans less than 300 km in diameter.

3. Steep middle-fan and lower-fan gradients.

These differences are interpreted as evidence of ice streams traversing the continental shelf and discharging sediment directly to the outer continental shelf and upper continental slope at times of glacial maxima.

The physiography of the Antarctic margin is unique, and the Wilkes Land margin

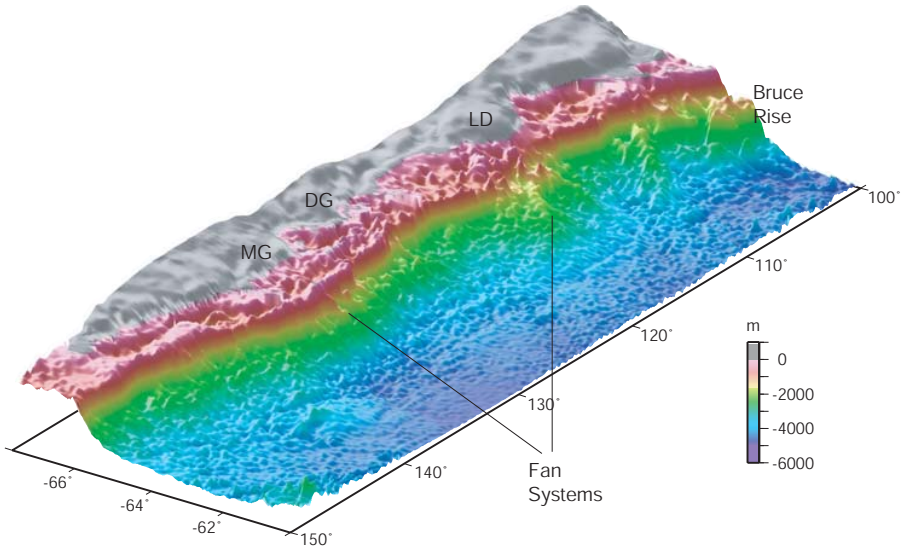

Figure 2.14: Perspective view, from the northeast, of the Wilkes Land margin physiography. The rugged topography of the shelf, comprising a number of deep canyons, is evident. The Bruce Rise forms a physiographic barrier at the western extreme of Wilkes Land. High relief sediment banks/ridges and deep canyons/channels define glacial sourced turbidite fan systems. Bathymetry from Smith & Sandwell [1994].

exhibits all of the characteristics that make it so. In addition, dynamic glacial conditions through the late Tertiary resulted in the creation of large fan systems on the Wilkes Land margin, similar in geometry to river-sourced fans, but of much greater magnitude.

2.11.2 Previous Marine Geophysical and Geological Data

Regional marine geophysical data acquired by Lamont-Doherty Geological Observatory, aboard the R/V Eltanin and Vema, 1968-1976, include bathymetric, gravity, and magnetic anomaly data from the southeast Indian Ocean, and the conjugate Australian-Antarctic margins (e.g. Weissel & Hayes [1972] and König & Talwani [1977]). These data were important in defining the broad structure of the Australia-Antarctic Basin (AAB), recognising the Australian-Antarctic Discordance (AAD), identifying Magnetic Quiet Zones (MQZ) at the continental margins, and timing the breakup of Australia and Antarctica.

Surveying since this time has tended to concentrate on the margins of Australia and Antarctica, and has included the acquisition of multi-channel seismic (MCS) data, in addition to gravity and magnetic anomaly data. The Wilkes Land margin has been surveyed sporadically since the 1980's, large portions of the margin, however, remain entirely unexplored.

The Australian-Antarctic Discordance (AAD)

The Australian-Antarctic Discordance (AAD) [Hayes & Conolly, 1972] is the portion of the Southeast Indian Ridge (SEIR) from ∼120-128°E that differs markedly in its morphologic and physical properties from the ridge flank areas immediately adjacent [Weissel & Hayes, 1972, 1974] (Figure 2.15). The AAD is characterised by extremely rugged ridge flank morphology, and closely spaced, north-south oriented fracture zones. Weissel & Hayes [1974] observed that the bathymetry of the SEIR flanks does not conform to depths expected given a simple lithospheric thermal contraction model for either the cooling plate or cooling half-space models (e.g. Parsons & Sclater [1977]. The depth of the SEIR itself is also anomalous, ∼1 km deeper than expected [Veevers, 1982].

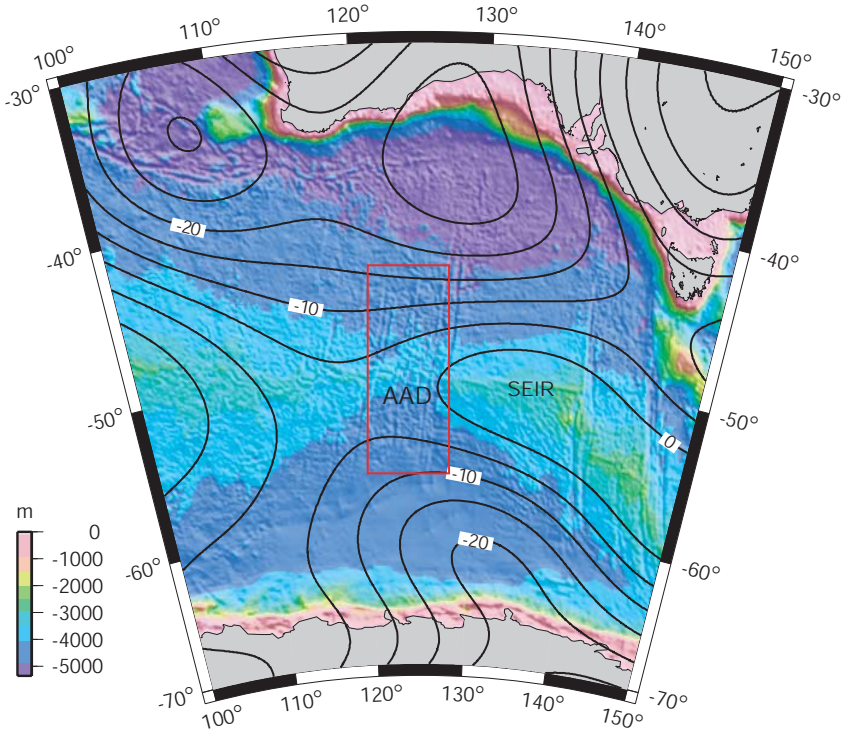

Figure 2.15: The southeast Indian Ocean between Australia and Antarctica. A broad bathymetric depression, centred on the Australian-Antarctic Discordance (AAD), is co-extensive with a broad negative anomaly in the long wavelength ($\lambda \gtrsim 2000$ km) free air gravity field (black contours). A saddle in the gravity field corresponds to the location of the AAD. Gravity contours from the model of Rapp & Pavlis [1990] and bathymetry from Smith & Sandwell [1994].

Thermal contraction models (e.g. Sclater & Francheteau [1970]) of the lithosphere predict that depth of oceanic crust is a function of age, and that crust of equal age should lie at equal depth in all ocean basins. Studies of the bathymetry of the world's ocean

basins broadly validate these models (e.g. Parsons & Sclater [1977]). However, relative to predicted depth, the Indian and Antarctic plates form a distinct regional negative depth anomaly in the region of the AAD. Maximum anomalies of 600-900 m were defined by Weissel & Hayes [1974], and anomalies in excess of 1000 m have been suggested more recently (e.g. Gurnis & Müller [2003]). The ∼2000 km wide depression extends at least 900 km from the ridge crest.

More extensive bathymetric compilations allowed Veevers [1982] to determine the regional extent of the AAD beyond the immediate area of the SEIR. Veevers [1982] defined a *"morphotectonic depression"* centred on the AAD, covering $\sim 15 \times 10^6$ km^2, that extended from the southern half of Australia to the Wilkes Land sector of Antarctica. The depth anomaly (i.e. the observed depth less the calculated depth based on a cooling plate model) of the southeast Indian Ocean is characterised by a linear, north-south trending depression, which traverses the AAB from the southern Australian margin to the Wilkes Land margin, Figure 2.16. The depth anomaly is approximately symmetrical with respect to the SEIR, which suggests the anomaly is a function of plate forming conditions at the ridge. The largest magnitude depth anomalies (>1000 m) are located close to the Australian and Antarctic margins, not at the ridge itself [Gurnis & Müller, 2003]. The AAD is, with respect to global residual oceanic bathymetry, the most prominent negative bathymetric anomaly not associated with present-day subduction [Gurnis *et al.*, 1998].

Figure 2.16: Residual topography of the southeast Indian Ocean and the Australian-Antarctic Discordance. Coloured dots represent isotopic signature of the mid-ocean ridge basalts, yellow = Pacific Ocean mantle, red = Indian Ocean mantle. Dotted line is the hypothesised trace of the isotopic boundary. Figure from Gurnis & Müller [2003].

Veevers [1982] demonstrated that the depression is co-extensive with a negative satellite free air gravity anomaly, as suggested by Weissel & Hayes [1974]. Comparison of the long wavelength gravity field ($\lambda \gtrsim 2000$ km) and the bathymetry of the southeast Indian Ocean illustrates the correlation between a saddle in the free air gravity and the location of the AAD (Figure 2.15). Although this saddle represents a relative high over the ridge, the gravity field is almost entirely negative. This contrasts with most mid-ocean ridges

where a positive free air gravity anomaly, with a wavelength of 2000-5000 km, is typically observed [Lambeck, 1972]. Weissel & Hayes [1974] suggested that the saddle in the gravity field reflects the combined effect of a typical mid-ocean ridge, and of the regional bathymetric depression.

Hayes & Conolly [1972] suggested that the observed depth anomalies are associated with a downwelling convective current in the asthenosphere. This interpretation was later supported by Weissel & Hayes [1974] and Veevers [1982] who also cited the negative, long wavelength free air gravity anomaly as evidence of downwelling mantle. Major element concentrations indicate that basalts from the AAD are consistent with lower than normal mantle temperatures [Klein & Langmuir, 1987].

Gurnis *et al.* [1998] suggest that the AAD is unique in being the only section of the present-day mid-ocean ridge system that intersects an ancient subduction zone. Gurnis & Müller [2003] infer that the SEIR, in the region of the AAD, intersects at depth lithosphere subducted by the long-lived Gondwana-Pacific/Phoenix convergent margin system. Global shear wave velocity models (e.g. Ritsema *et al.* [1999]) show a north-south trending high-velocity anomaly beneath the AAD, which Gurnis & Müller [2003] cite as evidence to support the Mesozoic subduction model for the origin of the AAD. Geochemical analyses also suggest a major change in asthenospheric-lithospheric source at the AAD, as it broadly marks the transition in tracer chemistry from 'Pacific Ocean type', to the east of the AAD, to 'Gondwana type', west of the AAD [Gurnis *et al.*, 1998] (Figure 2.16).

Antarctic and Southern Australian Margin Magnetic Quiet Zones (MQZ)

Weissel & Hayes [1971] first identified a magnetic quiet zone (MQZ) that *"begins just seaward of the continental slope and extends towards the land across the eastern continental margins of Antarctica and Australia"*. Weissel & Hayes [1972] defined the MQZ as regions where the amplitudes of local magnetic anomalies are extremely small. The seaward boundary of the MQZ is interpreted to cross-cut seafloor spreading anomalies, this indicates that the MQZ boundary itself is unlikely to be an isochron and is time-transgressive in some way Weissel & Hayes [1972].

Weissel & Hayes [1972] interpret the Antarctic MQZ to *"...presumably..."* occur over oceanic crust, and the Australian MQZ to be located both over oceanic crust and transitional crust beneath the lower continental slope. Various hypotheses have been considered to explain the origin of MQZ (e.g. Poehls *et al.* [1973]), however, König & Talwani [1977] find that these are not satisfactory to explain the presence of the Australian MQZ. They conclude that the crust below the MQZ is not typical oceanic crust. They suggest that

the crust is either:

1. Oceanic, but was never strongly magnetised or the magnetisation has been destroyed by some process since emplacement, or

2. Continental, with a low intensity of magnetisation.

Cande & Mutter [1982] used seafloor spreading modelling to demonstrate that the anomaly previously identified as chron 22 by Weissel & Hayes [1972] could be better modelled as chron 34. This revised interpretation did not require or preclude the presence of oceanic crust beneath the MQZ, and Cande & Mutter [1982] did not depart from the modes of origin suggested previously by König & Talwani [1977]. Veevers [1986], however, interpreted the MQZ to be floored by oceanic crust, as he suggested the landward boundary of the MQZ, the quiet zone boundary (QZB), represented the COB. Tikku & Cande [1999] question the validity of the interpretation of Veevers [1986], as it is unclear that the anomaly correlates directly with the COB for the entire span of the AAB.

Magnetic and gravity modelling by Sayers *et al.* [2001], based on seismic reflection data, and interpretation of seismic reflection data suggests that the Australian MQZ is floored by stretched continental crust. The COB in the model of Sayers *et al.* [2001] occurs farther seaward than previous interpretations. They, therefore, question the validity of identifying oceanic crust on the basis of magnetic anomalies only.

Seismic Reflection Data

Surveys focused on acquiring geophysical data along sections of the Wilkes Land margin were first carried out in the early 1980's by the IFP, JNOC and USGS. Each survey acquired seismic reflection, gravity anomaly, and magnetic anomaly data. Interpretations of these data, carried out independently by the individual institutions, broadly identified similar stratigraphic seqeunces. However, interpretation of the COB location, on the basis of the seismic character of the crust, differed significantly. More recent surveys have been completed by the JNOC (1993-94-95), and the Wilkes Glacial history (WEGA) project [De Santis *et al.*, 2003].

During the austral summer of 1982, the IFP survey ATC82 acquired ~3000 line-km of data off the east Wilkes Land-Terre Adélie margin, 136-154°E [Wannesson *et al.*, 1985]. Survey lines extended from the inner continental shelf (due to favourable ice conditions during the survey period) to the abyssal plain of the AAB.

The JNOC conducted two surveys in the early 1980's, survey TH82 during the 1982-83 austral summer [Tanahashi *et al.*, 1987], and the more extensive survey TH83 the following austral summer [Tsumaraya *et al.*, 1985]. Survey TH82 acquired 680 line-km of MCS data off east Wilkes Land. The TH83 survey acquired ~3700 km of MCS data, from

108-140°E). The JNOC completed a further survey on the Wilkes Land margin during 1995, TH95 [Tanahashi *et al.*, 1997]. Dredge samples were recovered during survey TH95, which indicate a cluster of seamounts off the east Wilkes Land-Terre Adélie margin have a geochemical signature indicative of a continental mantle lithosphere source [Yuasa *et al.*, 1997].

During the austral summer of 1984, the USGS research vessel *S.P. Lee* completed a survey (L184) of the east Wilkes Land margin [Eittreim & Hampton, 1987]. Over 1800 line-km of MCS data were acquired on 14 lines, from 130-146°E, which were interpreted by Eittreim & Smith [1987] and Hampton *et al.* [1987]. Icebergs and sea ice limited the southern extent of the survey and only one line extended landward of the shelf break.

The seismic stratigraphic interpretations of Wannesson *et al.* [1985], Tanahashi *et al.* [1987], Tsumaraya *et al.* [1985], and Eittreim & Smith [1987] were broadly similar. The interpreted number of sequences varied between interpretations, however, major unconformities were recognised that can be correlated. The inferred ages of unconformities, and nomenclature for their labelling, adopted during each interpretation was different. This prompted Tanahashi *et al.* [1994] to introduce a uniform nomenclature, for the major unconformities that were similarly interpreted within each data set. Figure 2.17 summarises the sequence stratigraphy of each of the above workers and correlates them to the uniform nomenclature introduced by Tanahashi *et al.* [1994]. Data acquired during survey TH95 were interpreted using the framework introduced by Tanahashi *et al.* [1994].

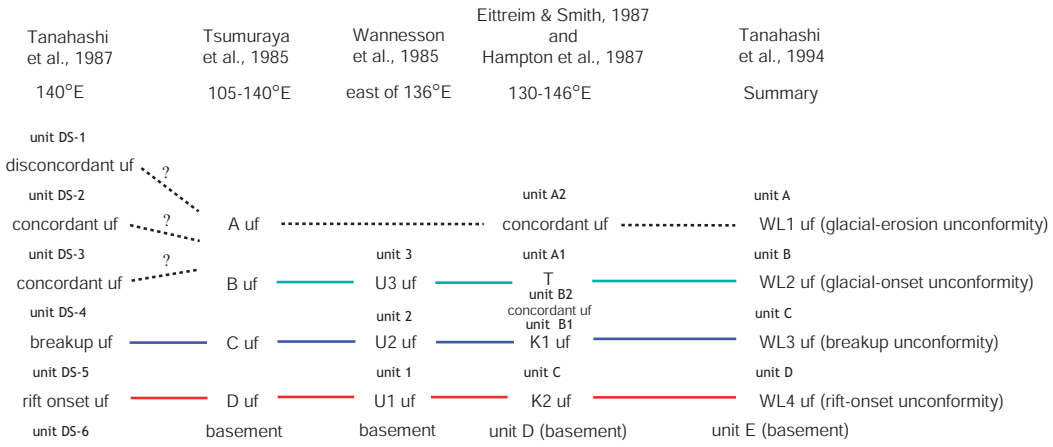

Figure 2.17: Summary of the seismic stratigraphic interpretations of MCS data acquired on the Wilkes Land margin. The summary of Tanahashi *et al.* [1994] includes the formative mechanism of the interpreted unconformities (uf).

Seismic reflection data were ubiquitously interpreted to indicate an absence of large-scale volcanism associated with rifting and breakup on the Wilkes Land margin. Various amounts of volcanism were interpreted, however, no evidence of seaward dipping reflec-

tor sequences or flood basalts was identified. Previous interpretations of the conjugate southern Australian margin had concluded that it too was non-volcanic, hence, the absence of extensive volcanism on the Wilkes Land margin had been previously predicted on this basis.

Despite the broad agreement in the interpretation of the major sedimentary sequences, widely varying estimates of the COB location and the crustal type beneath the MQZ were suggested on the basis of seismic interpretation. *Moho* reflections were interpreted in data from ATC82 and L184 data, however, relatively few strong reflections from within the crust were recorded. Hence, there is very little contrast in the recorded seismic character of the oceanic and continental crust surveyed. A basement rise off the east Wilkes Land-Terre Adélie margin added a degree of complexity to the interpretations. Sections of this high were traversed by the ATC82, TH83, L184, and TH95 surveys.

The basement high was interpreted by Wannesson *et al.* [1985] as oceanic crust, they cited the continuity of a reflector, interpreted as the *Moho*, beneath the high as evidence of oceanic crust. Hence, they interpreted the MQZ to be floored by oceanic crust, and that the lack of anomalies is due to emplacement during the Cretaceous normal polarity epoch. They interpret a COB adjacent to the foot of the continental slope. Tanahashi *et al.* [1987], in contrast, interpret the basement high to represent stretched continental or 'transitional' crust. Hence, the COB interpreted by Tanahashi *et al.* [1987] is located over 400 km seaward of that interpreted by Wannesson *et al.* [1985]. Eittreim & Smith [1987] interpret the basement high to represent volcanic build-ups associated with the earliest emplacement of oceanic crust. Hence, their interpreted COB is located at the landward edge of the high, between the interpretations of Wannesson *et al.* [1985] and Tanahashi *et al.* [1987]. Other geophysical evidence, such as potential field data and limited heat flow and sonobuoy refraction data, was not sufficient to resolve the differences in interpretation.

Seismic reflection data from survey TH95 images >1 s two-way-time (TWT) of deformed sediments overlying a section of the basement high. This was interpreted to confirm the presence of transitional crust and a COB seaward of the basement high [Tanahashi *et al.*, 1997]. Additionally, the geochemistry of dredge samples recovered from a seamount in the region were interpreted by Yuasa *et al.* [1997] to indicate that active seafloor spreading initiated seaward of the seamount location. Thus, indicating that the basement high comprises, and the majority (if not all) of the MQZ is floored by, stretched continental or transitional crust.

2.12 Summary

Relative to all other continents, the study of Antarctica has a short history. Antarctica is also the only continent where surface geological mapping is limited to less than 2% of the continental surface. These factors, combined with the absence of resource exploration and exploitation, explain why there are still many unanswered questions with regard to the geology and tectonics of Antarctica. However, much has been achieved and many important discoveries made since scientific surveying began in the early 1900's.

The Wilkes Land margin remains one of the least explored marine sectors of Antarctica. The sediment thickness and crustal structure are poorly constrained for much of the region. Surveys that have explored this margin define a number of interesting features with regards to the influence of glaciation on the physiography and sedimentation patterns on the margin. The composition and origin of basement features and the location of the COB off the Wilkes Land margin remains enigmatic. This contrasts with the conjugate southern Australian margin, which has been the subject of relatively intense study for many decades. The geological evolution and structural architecture of the Wilkes Land margin is, therefore, of great interest. Investigations of this conjugate margin pair provides a basis for further understanding the evolution of non-volcanic, passive rift margins.